Pellet Injectors for JET

C. Andelfinger, K. Büchl, R.S. Lang
H.B. Schilling, M. Ulrich

IPP 1/193 Sept.1981

MAX-PLANCK-INSTITUT FÜR PLASMAPHYSIK
8046 GARCHING BEI MÜNCHEN

MAX-PLANCK-INSTITUT FÜR PLASMAPHYSIK

GARCHING BEI MÜNCHEN

Pellet Injectors for JET

C. Andelfinger, K. Büchl, R.S. Lang
H.B. Schilling, M. Ulrich

IPP 1/193 Sept.1981

This work was done under contract JB1/9005

The material for this report was prepared by the IPP staff members:
W. Amenda, C. Andelfinger, K. Büchl, E. Buchelt, D. Jacobi, H. Kollotzek, R.S. Lang, E. Lackner, Th.v.Larcher, G. Prausner, H.-B. Schilling, M. Ulrich, G. Weber.

Max-Planck-Institut für Plasmaphysik
EURATOM - Association, D-8046 Garching

Die nachstehende Arbeit wurde im Rahmen des Vertrages zwischen dem Max-Planck-Institut für Plasmaphysik und der Europäischen Atomgemeinschaft über die Zusammenarbeit auf dem Gebiete der Plasmaphysik durchgeführt.

IPP 1/193

C. Andelfinger,
K. Büchl,
R.S. Lang,
H.B. Schilling,
M. Ulrich

Pellet Injectors for JET

September 1981

Abstract

Pellet injection for the purpose of refuelling and diagnostic of fusion experiments is considered for the parameters of JET. The feasibility of injectors for single pellets and for quasistationary refuelling is discussed. Model calculations on pellet ablation with JET parameters show the required pellet velocity ($\leq$ 2000 m/s) and size ($\leq$ 50 mm^3). For single pellet injection a light gas gun, for refuelling a centrifuge accelerator is proposed. For the latter the mechanical stress problems are discussed. Control and data acquisition systems are outlined.

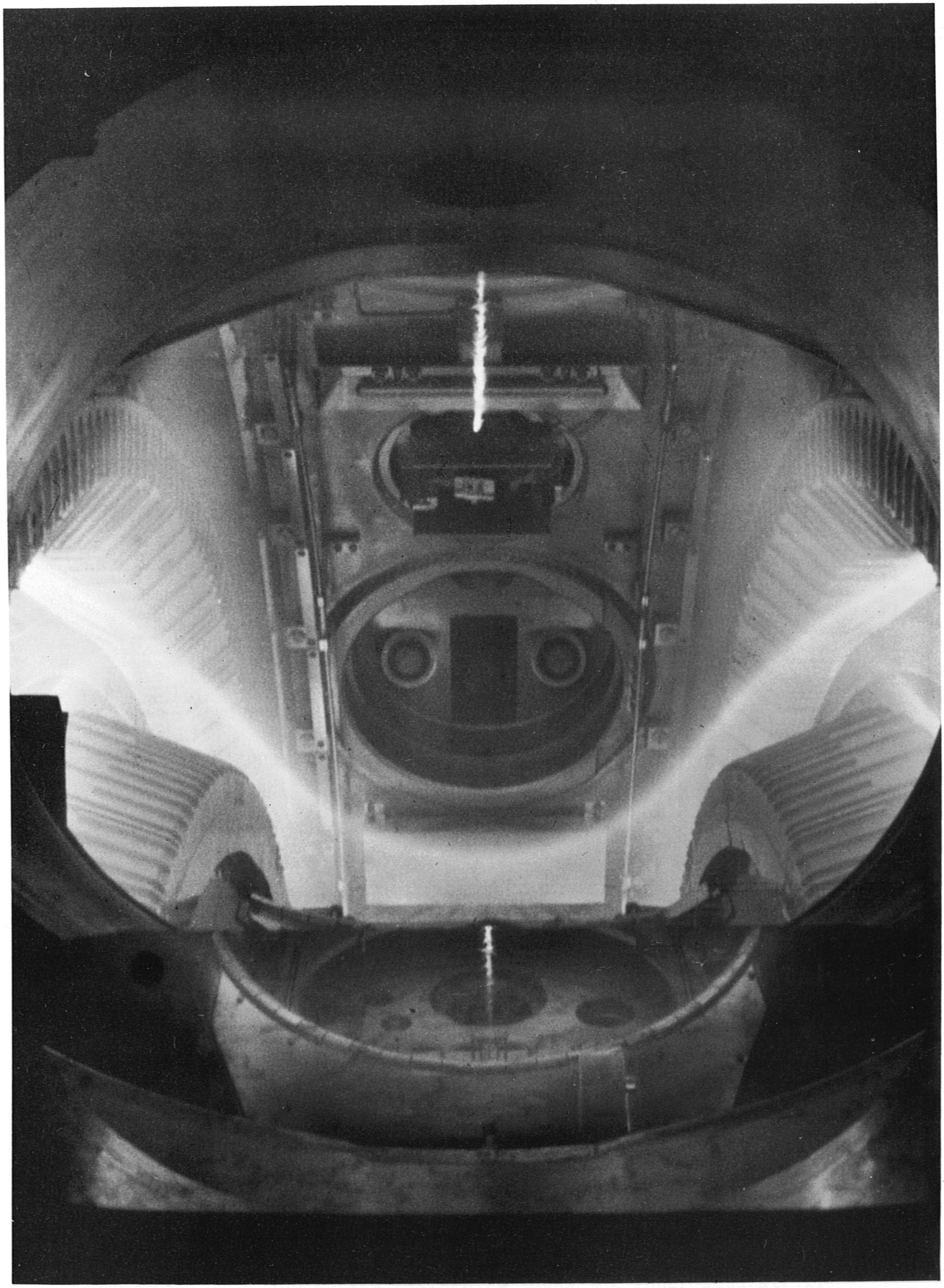

Contents

Cover picture: Pellet Path in an ASDEX Discharge
The curved blackening shows the inner separatrix, the upper path was seen via a mirror

Pellet Injectors for JET

1. Introduction

The injection of high-speed pellets of frozen hydrogen or hydrogen isotopes was seen as a method of refuelling fusion experiments, being first proposed by Spitzer in 1954 /1/. Successful experiments with ISX-A and ISX-B /2/ have shown that it is also a suitable method for achieving a sudden increase of the plasma density, as required for a dense target plasma in experiments with neutral injection and for long energy and particle confinement times. A further advantage compared with cold gas inlet will be that one can probably influence the density profile of the plasma, especially in its outer region, by varying the pellet size and/or pellet velocity.

The transport of impurities could be investigated by injecting neon-contaminated D_2 pellets, which can be produced with the same apparatus.

For all these purposes pellet injectors are needed which allow variation of the pellet velocity, pellet frequency and pellet size.

It would be advantageous to do the first investigations with two independent single-pellet injectors such as light-gas guns. Their development is more advanced than centrifuge accelerators. Such experiments deliver information about the range, ablation, resulting density profile, particle confinement time, and desirable pellet frequency for stationary refuelling. Single-pellet injection may help to produce the desired target plasma for neutral injection. After this learning period a centrifuge accelerator should be available for quasistationary refuelling. With this kind of injector we still have problems with the introduction of the pellets into the centrifuge, which mainly determines the angular spread of the accelerated pellets. Modern composite materials with high strength-to-weight ratio should render possible pellet velocities of up to 2000 m/s.

No complete theoretical treatment of the pellet penetration and ablation is available. Especially the influence of fast runaway electrons as well

as anisotropic fast ions resulting from neutral injection are not considered. Experiments up to now best fit the so-called "shielded pellet neutral evaporation" based on the theory of Parks, Turnbull and Foster /3/, modified by Milora and Foster /4/. This model was used for calculating pellet ablation and penetration in assumed JET plasmas. The results are presented in the next section.

2. Model Calculations for Ablation, D_2 Deposition, Density and Temperature Profiles and Penetration of Pellets in Assumed JET Plasmas

Reviews of the present ablation theories are given by Milora / 2 / and Chang et al. / 5 /. The neutral shielding model is the best approximation to the previous experiments. The proposed JET plasma with ohmic heating (OH) and with neutral injection of the first step (NI 1) probably meets the conditions for the application of this model. Interaction of pellets with runaway electrons as well as changes of plasma properties influenced by ablation itself (internal disruptions, instabilities, anomalous transport) are neglected. The only heat source of pellets should be the Maxwellian electrons. Ablation due to fast ions from neutral injection is not considered either. The pellets are assumed to be spherical.

Houlberg et al. / 6 / published an ablation code including the finite energy content of the plasma confined in cylindrical shells. We are using this code with temperature and density profiles given by JET to calculate the deposition profile (ablated atoms per cm path) and the changed density and temperature profiles. The temporal developments of these profiles are not considered; this has to be done with a transport code.

The radius of the spherical pellets will be varied between 1.0 mm and 3.5 mm. The relation between the number of atoms in spherical and cylindrical pellets and the number of ions in the JET plasma can be taken from fig. 1 . A plasma density of 2×10^{19} m^{-3} is assumed. The calculations are done for D_2 pellets because the production of D_2 pellets entails fewer problems than the production of H_2 pellets.

The pellet velocities used in the calculations are 300, 600, 900, 1200, and, in some cases, 1500 and 2000 m/s. Today the maximum pellet velocity attained is 1000 m/s in several experiments.

The following plasma profiles are assumed:

OH operation

$$n_e = 2 \times 10^{19} \, [1 - (r/a)^8] + 6 \times 10^{18} \, [m^{-3}]$$

$$T_e = 1 \times 10^3 \, [1 - (r/a)^2]^{2.5} + 50 \, [eV]$$

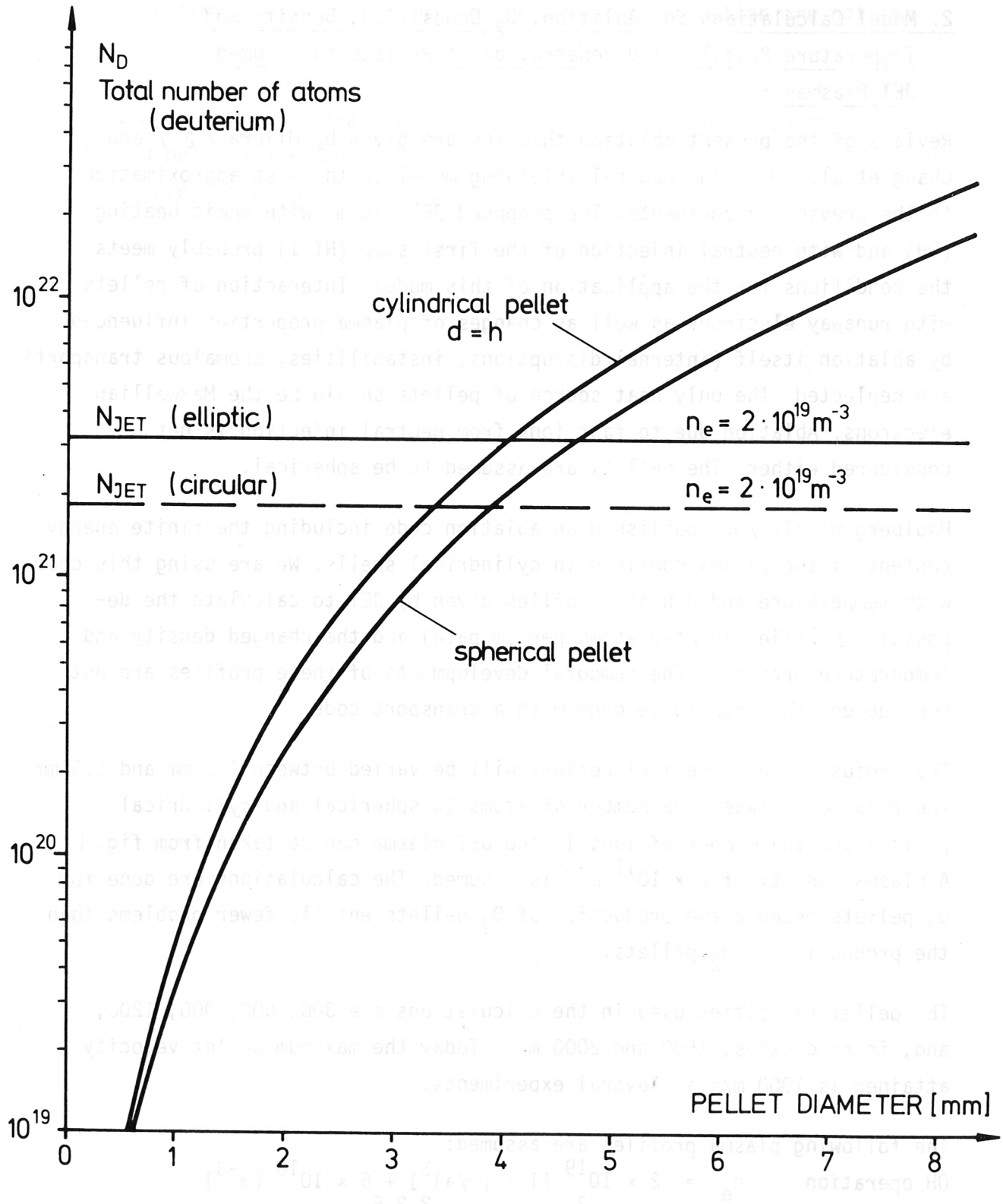

Fig.1 Number of atoms versa pellet diameter

NI-1 operation	n_e = 4×10^{19}	$[1 - (r/a)^8] + 8 \times 10^{18}$ $[m^{-3}]$
	T_e = 2×10^3	$[1 - (r/a)^2]^{2.5} + 50$ [eV]
NI-2 operation	n_e = 9×10^{19}	$[1 - (r/a)^8] + 10 \times 10^{18}$ $[m^{-3}]$
(extended version)	T_e = 6×10^3	$[1 - (r/a)^2]^{2.5} + 50$ [eV]

The boundary values of n_e and T_e are arbitrary, but they have no strong influence on the ablation. T_e at the torus axis is chosen conservatively to be about one-third of the maximum value given by JET. Owing to all the restrictions the calculated profiles will be only rough approximations to the experiments. However, the model calculations can be used for discussion of pellet size and velocity to be applied in JET.

We consider an elliptical plasma cross-section with horizontal injection and choose a relation of pellet mass to plasma mass of 20 to 100 %. For such relations pellets were injected without disruptions into Pulsator, W VIIA, ASDEX and ISX-B / 2/. This means a pellet radius of 1.5 mm to 2.5 mm for JET. By varying the pellet velocity the complete range from edge deposition to near-axis deposition can be covered. This will be possible for OH operation with pellet radius of 1.0 to 1.5 mm. 2 mm pellets completely penetrate the plasma for high velocities and are unsuitable for refuelling. With axis temperatures of 2 keV (NI-1 operation) pellets of 2.0 to 2.5 mm radius are able to penetrate to the axis. Bigger pellets, however, will not ablate completely in the plasma for high velocities and should not be used in this operation. For the extended version of JET the neutral shielding model calls for much bigger pellets for near-axis deposition.All these conclusions are drawn by means of figures 2 - 8.
A compromise for OH and NI-1 operation is to start the experiments with pellets of 1.5 mm radius.

3. Single D_2 Pellet Injection with a Light-Gas Gun

3.1 Pellet production

The pellets will be produced in a conventional cryostat using heat exchange with flowing liquid helium (Fig. 9). At a temperature of about 8 K deuterium gas will be solidified in a store cavity which can house the material for

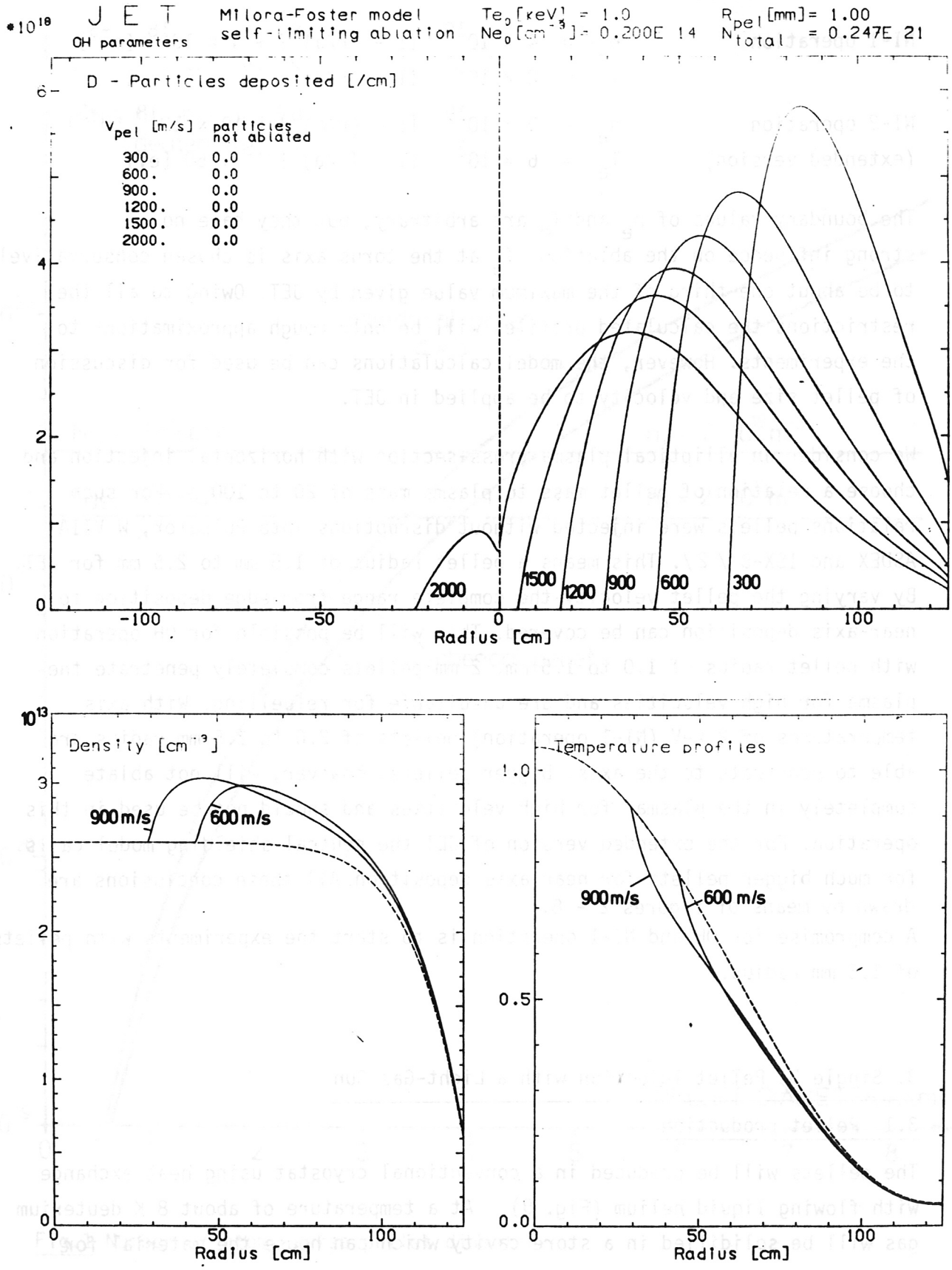

Fig.2 Particles deposition, density and temperature profile for Te_o = 1.0 keV, Ne_o = $2 \cdot 10^{13}$ cm^{-3} and R_{pel} = 1.00 mm

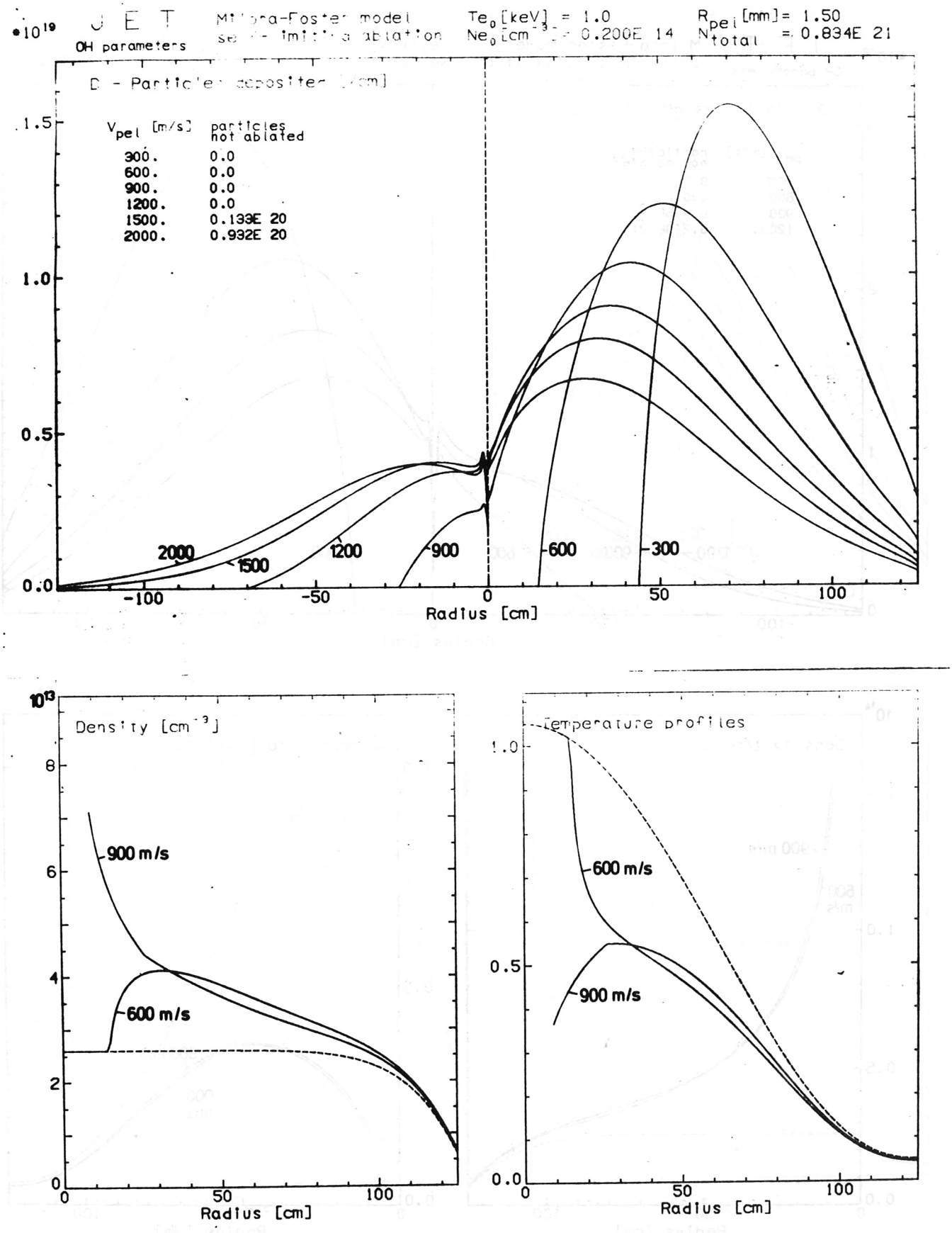

Fig.3 Particles deposition, density and temperature profile for Te_o = 1.0 keV, Ne_o = $2 \cdot 10^{13}$ cm^{-3} and R_{pel} = 1.5 mm

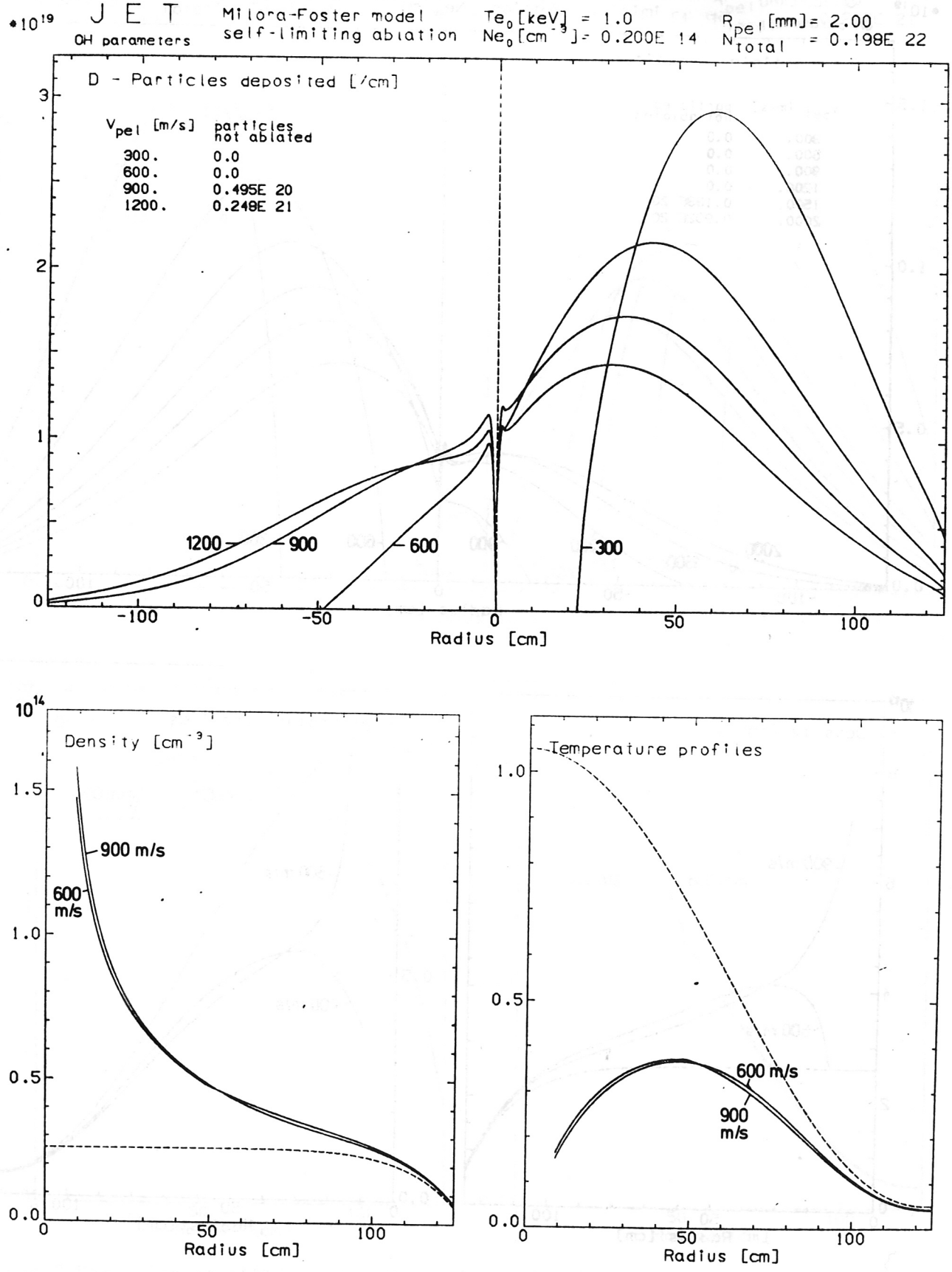

Fig.4 Particles deposition, density and temperature profile for Te_o = 1.0 keV, $Ne_o = 2 \cdot 10^{13}$ cm^{-3} and R_{pel} = 2.0 mm

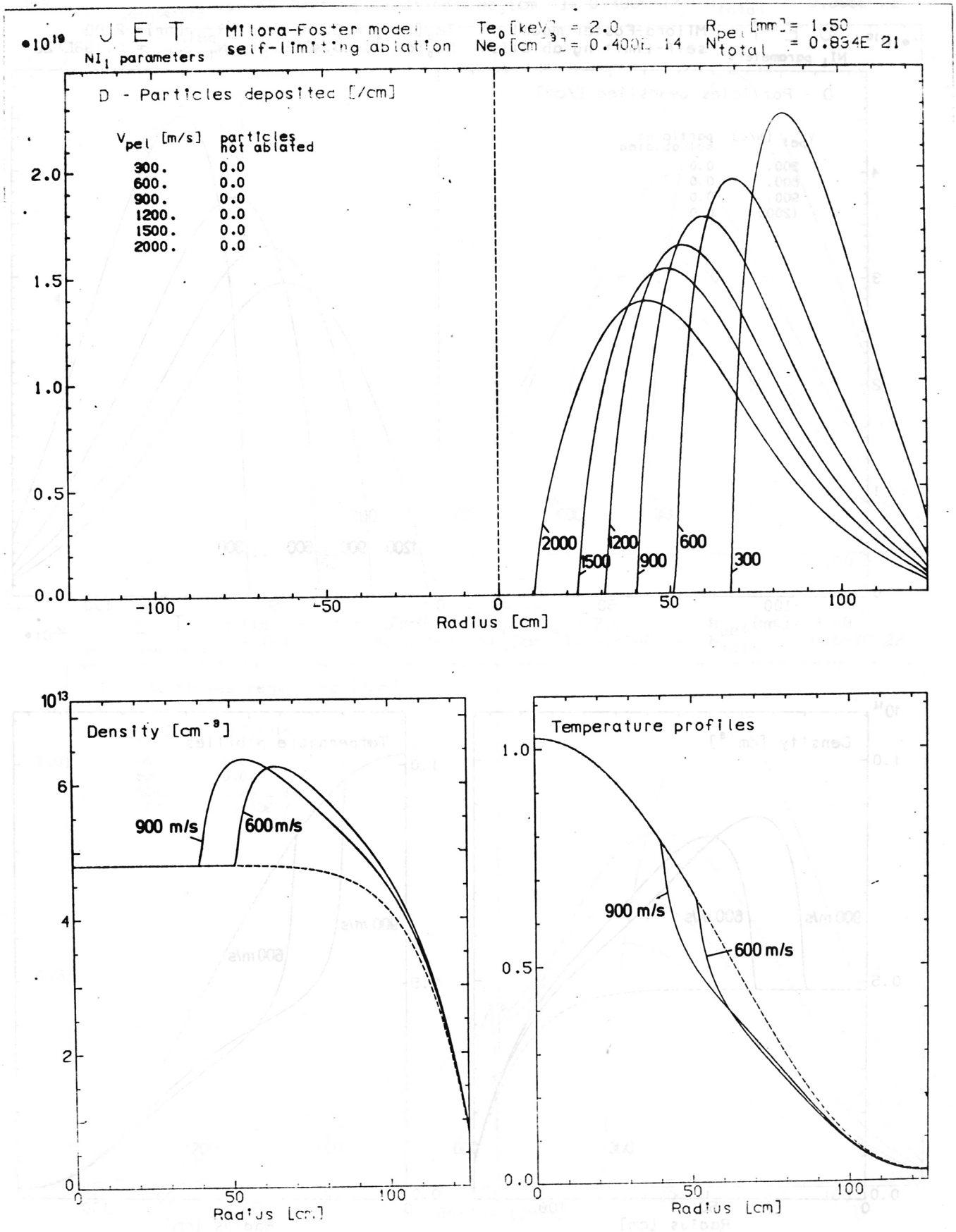

Fig.5 Particles deposition, density and temperature profile for Te_o = 2.0 keV, $Ne_o = 4 \cdot 10^{13}$ cm^{-3} and R_{pel} = 1.5 mm

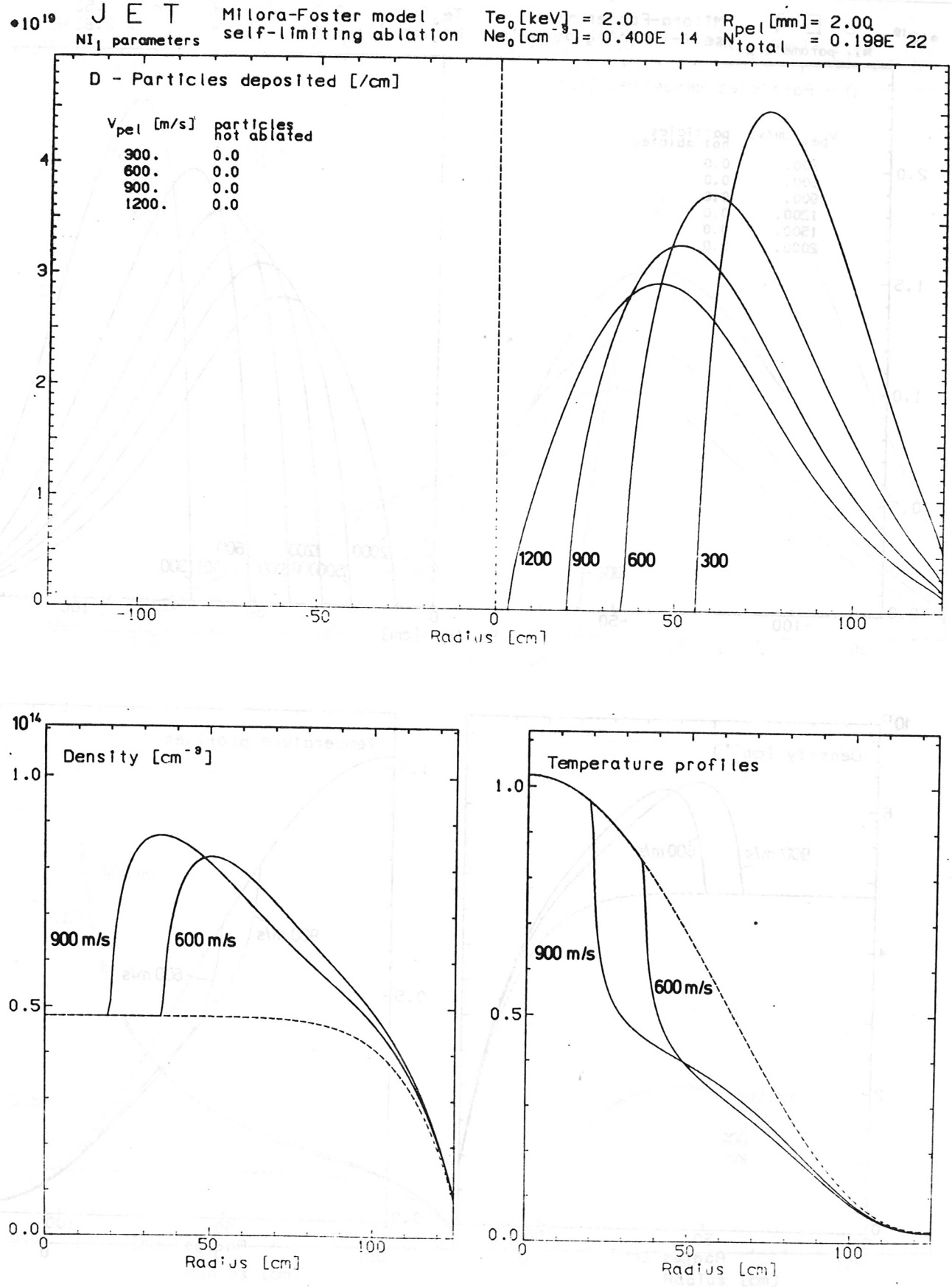

Fig.6 Particles deposition, density and temperature profile for Te_o = 2.0 keV, $Ne_o = 4 \cdot 10^{13}$ cm^{-3} and R_{pel} = 2.0 mm

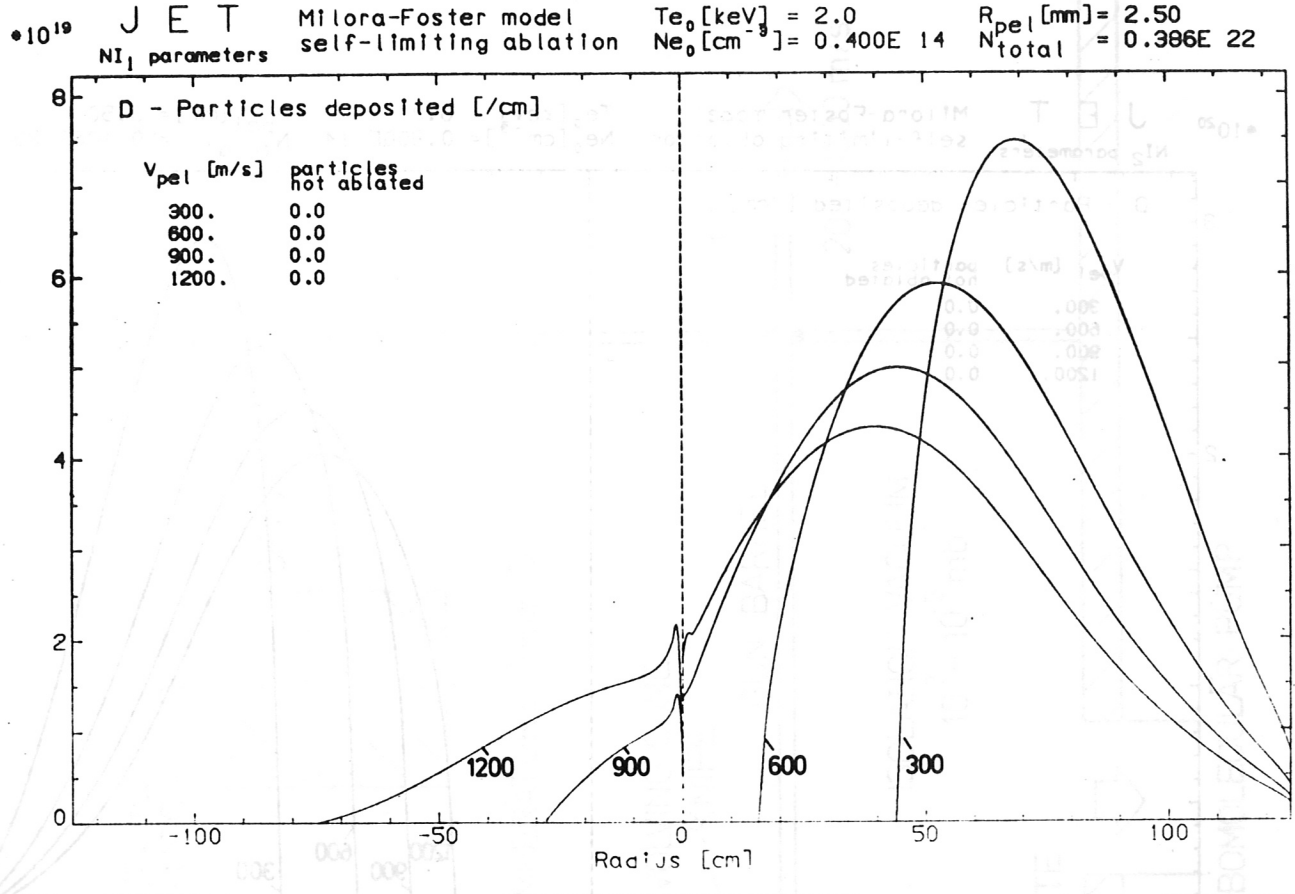

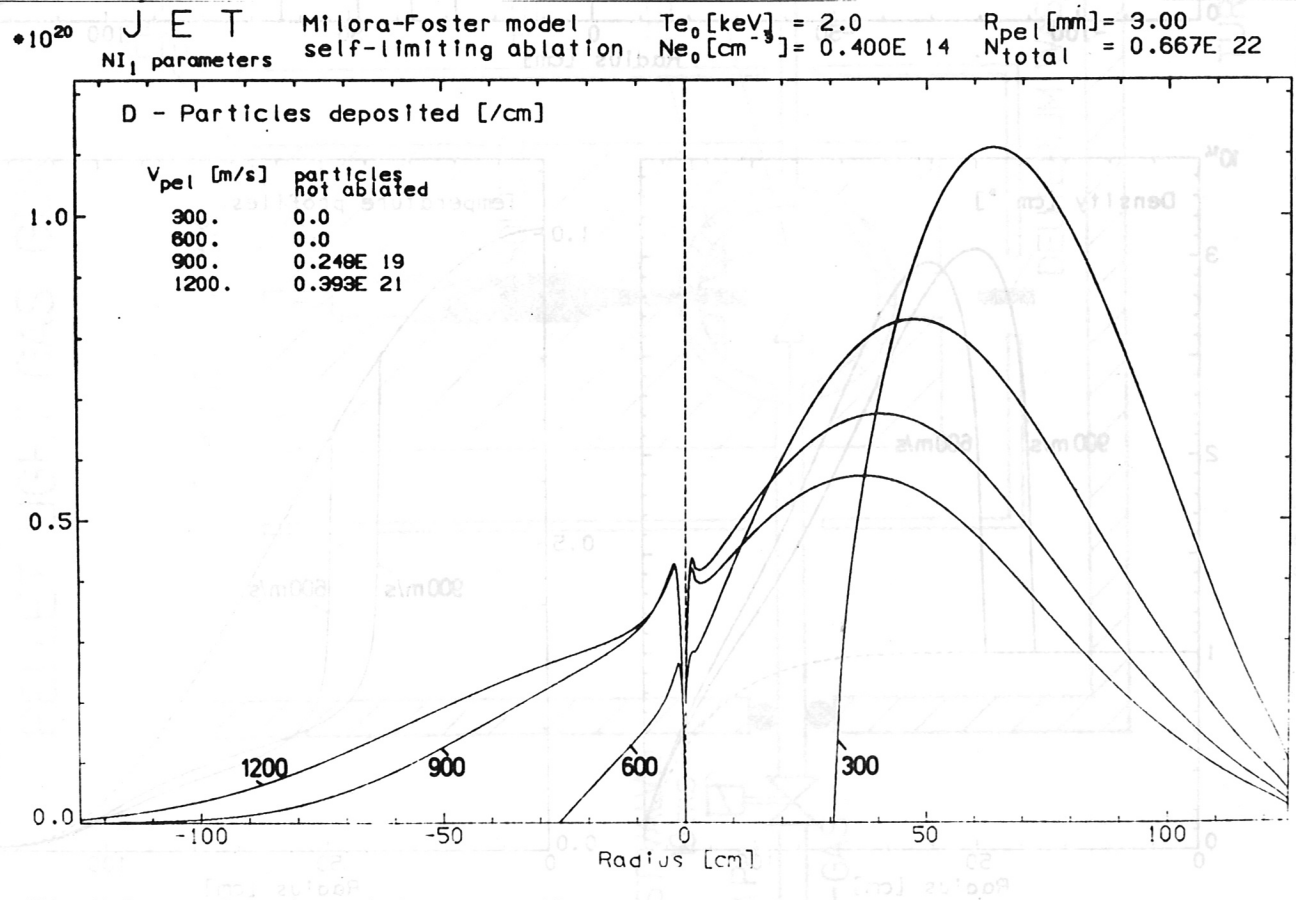

Fig.7 Particles deposition, profile for

Te_o = 2.0 keV, Ne_o = $4 \cdot 10^{14}$ cm^{-3} and R_{pel} = 2.5 mm and 3.0 mm

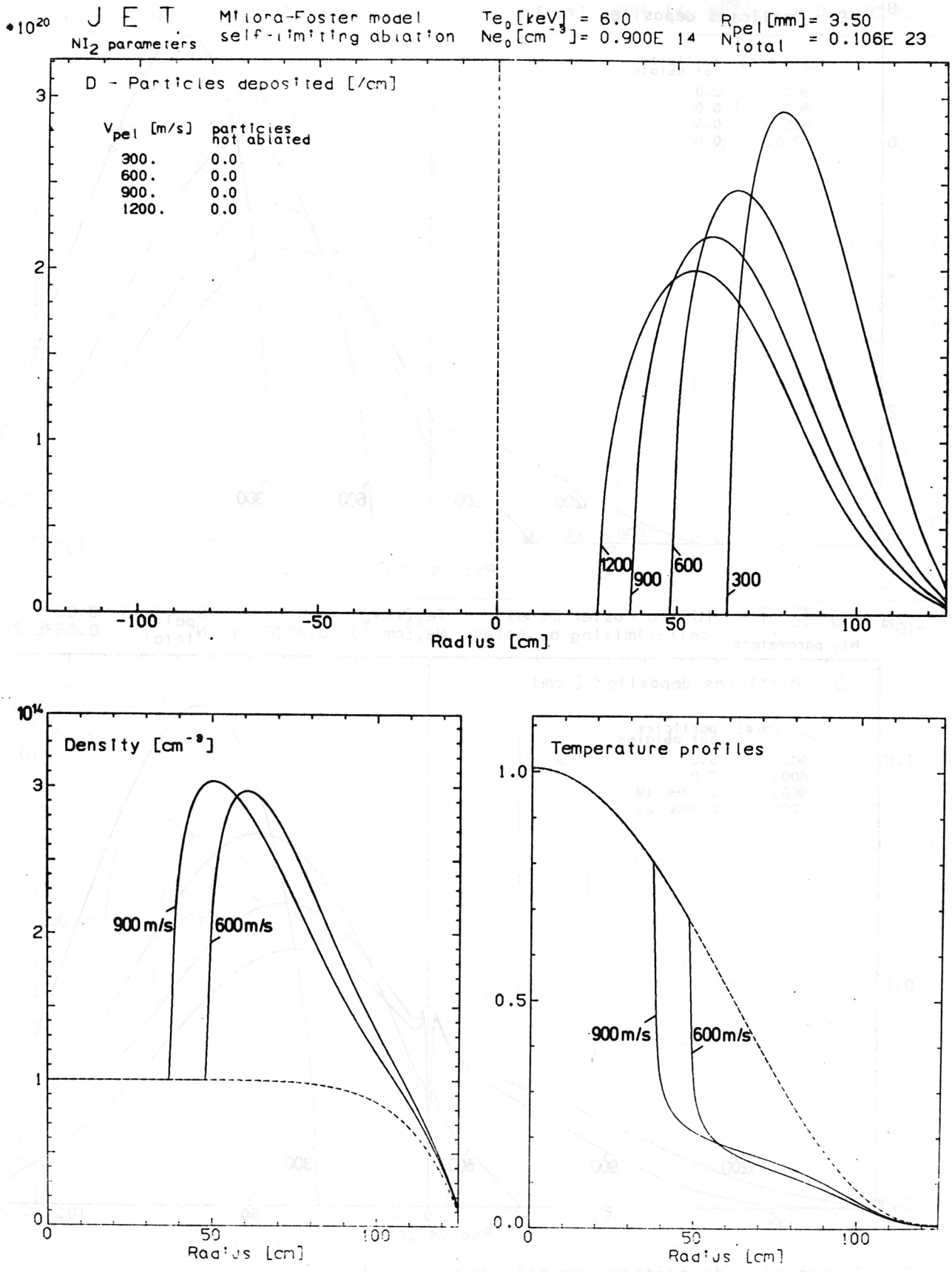

Fig.8 Particles deposition, density and temperature profile for Te_o = 6.0 keV, $Ne_o = 9 \cdot 10^{13}$ cm^{-3} and R_{pel} = 3.5 mm

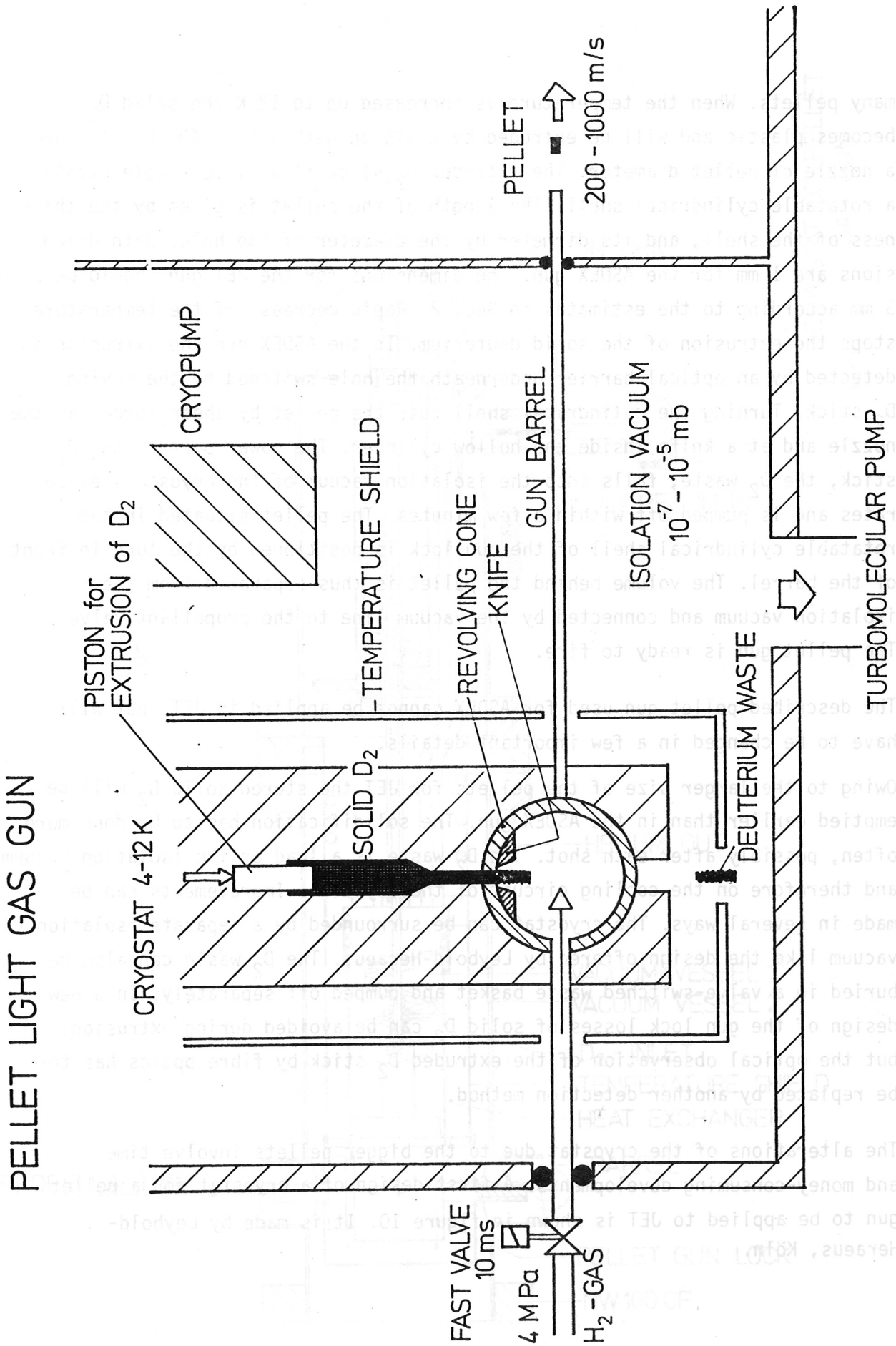

Fig.9 Principle of pellet light-gas gun

many pellets. When the temperature is increased up to 12 K the solid D_2 becomes plastic and will be extruded by a piston with 300 to 400 bar through a nozzle of pellet diameter. The extruded D_2 stick flows into a hole within a rotatable cylindrical shell. The length of the pellet is given by the thickness of the shell, and its diameter by the diameter of the hole. Both dimensions are 1 mm for the ASDEX gun. The dimensions for the JET gun should be about 3 mm according to the estimates in Sec. 2. Rapid decrease of the temperature stops the extrusion of the solid deuterium. In the ASDEX gun the extrusion is detected by an optical barrier underneath the hole switched by the moving D_2 stick. Turning the cylindrical shell cuts the pellet by shear forces at the nozzle and at a knife inside the hollow cylinder. The lower part of the D_2 stick, the D_2 waste, falls into the isolation vacuum of the cryostat, evaporates and is pumped off within a few minutes. The pellet situated in the rotatable cylindrical shell of the gun lock is positioned by the turn in front of the barrel. The volume behind the pellet is thus separated from the isolation vacuum and connected by the vacuum line to the propellant valve. The pellet gun is ready to fire.

The described pellet gun used for ASDEX cannot be applied in JET, but will have to be changed in a few important details.

Owing to the larger size of the pellets for JET the stored solid D_2 will be emptied earlier than in the ASDEX gun. The solidification has to be done more often, possibly after each shot. The D_2 waste is a load on the isolation vacuum and therefore on the cooling circuit of the cryostat. Improvements can be made in several ways. The cryostat can be surrounded by a separate isolation vacuum like the design offered by Leybold-Heraeus. The D_2 waste can also be buried in a valve-switched waste basket and pumped off separately. In a new design of the gun lock losses of solid D_2 can be avoided during extrusion, but the optical observation of the extruded D_2 stick by fibre optics has to be replaced by another detection method.

The alterations of the cryostat due to the bigger pellets involve time and money-consuming developments. A first design of a cryostat for a pellet gun to be applied to JET is shown in figure 10. It is made by Leybold-Heraeus, Köln.

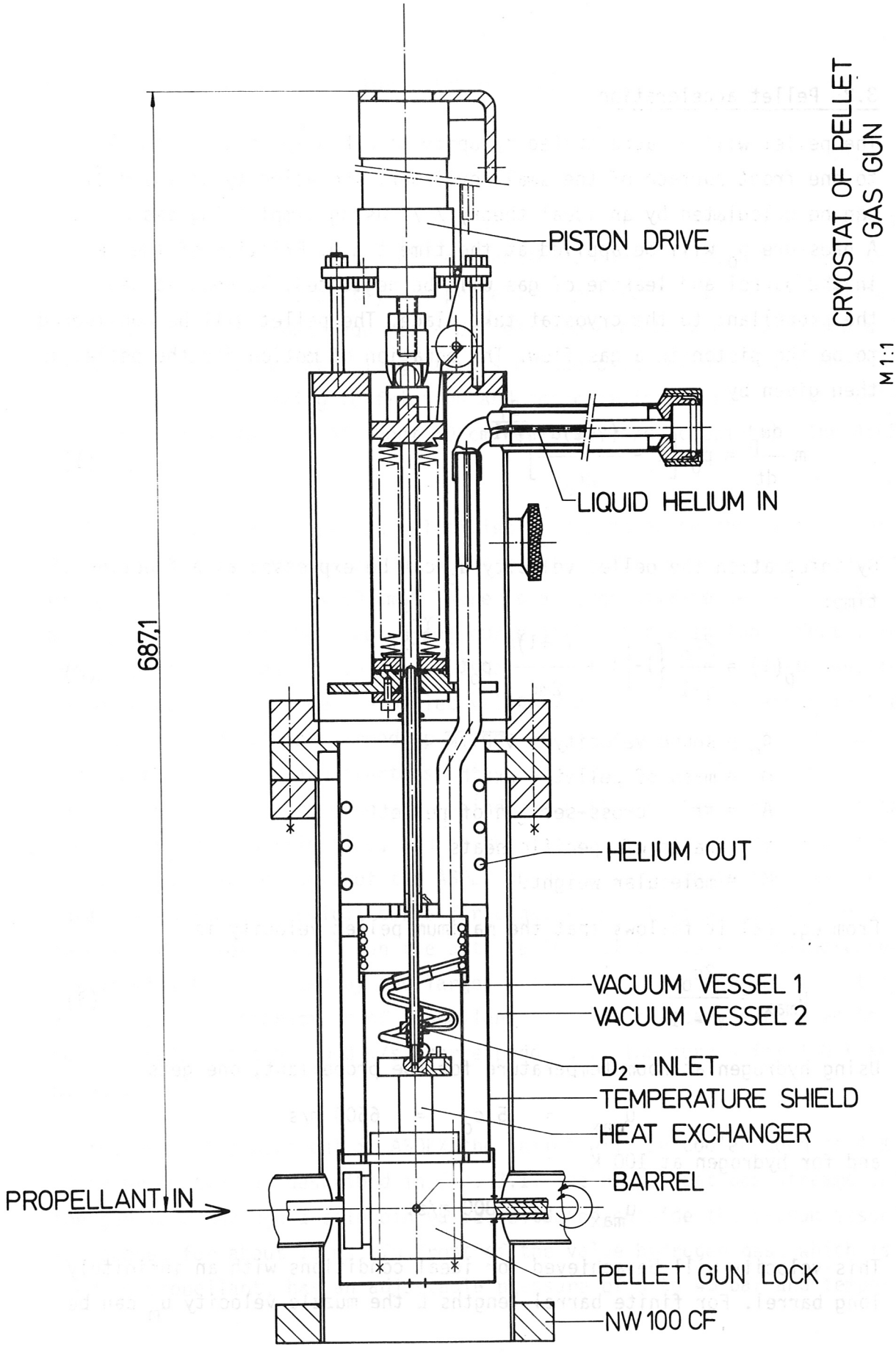

Fig.10 Preliminary design of the pellet light-gas gun (Leybold-Heraeus)

3.2 Pellet acceleration

The pellet will be accelerated by applying a high-pressure propellant to one front surface of the small cylinder. The velocity of the pellet can be calculated by an ideal theory / 7/ using simplifying assumptions. A pressure p_o will be applied at the time t = 0. Friction of the pellet in the barrel and leakage of gas will be neglected. No heat losses of the propellant to the cryostat take place. The pellet will be considered to be the piston in a gas flow. The equation of motion for the pellet is then given by

$$m \frac{du_p}{dt} = p_o \left[1 - \frac{(\gamma-1)u_p}{2c_o}\right]^{\frac{2\gamma}{\gamma-1}} \qquad (1)$$

By integration the pellet velocity u_p can be expressed as a function of time:

$$u_p(t) = \frac{2c_o}{\gamma-1}\left\{1-\left[1 + \frac{(\gamma+1)A}{2mc_o} p_o t\right]^{-\frac{\gamma-1}{\gamma+1}}\right\} \qquad (2)$$

c_o = sound velocity = $\sqrt{\gamma RT/M}$
m = mass of pellet = $\rho\pi r^2 h$
A = πr^2 cross-section of pellet
γ = ratio of specific heats
M = molecular weight.

From eq. (2) it follows that the maximum pellet velocity is

$$u_{max} = \frac{2c_o}{\gamma - 1} \qquad (3)$$

Using hydrogen at room temperature for the propellant, one gets

$$u_{max} = 5\, c_o = 6500 \text{ m/s}$$

and for hydrogen at 100 K

$$u_{max} = 3800 \text{ m/s}.$$

This velocity will be achieved for ideal conditions with an infinitely long barrel. For finite barrel lengths L the muzzle velocity u_m can be

calculated implicitly by integrating eq. (2):

$$L(u_m) = \int_0^{t_m} u_p(t)dt \qquad (4)$$

The pellet leaves the barrel at time $t = t_m$. In fig. 11 the pellet velocity is shown as a function of the barrel length for several pellet sizes, gas temperatures (sound velocity) and propellant pressures. To get velocities up to 1000 m/s, the gun requires a barrel length of between 10 cm and a few metres. For the experiment long barrels of the order of one metre could involve difficulties owing to friction and decrease in pressure of the propellant, and so lengths of about 50 cm would be more acceptable. The ASDEX guns use 35 cm.

In fig. 12 calculated pellet velocities u_m depending on the pressure of the propellant are shown for the ASDEX gun (h = 1.1 mm, L = 35 cm) and the JET gun (h = 3.0 mm, L = 50 cm). There is a large difference between the measured values and the theoretical curve at 300 K due to two effects. When the propellant streams into the cryostat, the gas will be cooled down. The sound velocity and hence the pellet velocity decrease. Simultaneously the cryostat itself will be warmed up by the propellant, so that the pellet becomes more plastic and starts shortly after opening of the propellant valve. However, the incoming gas behind the pellet has not yet reached the pressure p_o during this time, and so the pellet velocity is reduced once more. The corrected curve of the ASDEX gun is also shown in fig. 12 and agrees with the theoretical curve for a gas temperature of 40 K. With a longer barrel for the JET gun the attainable pellet velocity is increased, but it will be decreased by the larger pellet mass. For the JET gun it is hoped that the interaction of propellant and cryostat can be reduced to achieve velocities of 1000 m/s, corresponding to the curves for 100 K and higher.

In the present experiment in ASDEX the pellet will be cooled down to 4 K after production as described in Sec. 3.1. The propellant gas streams into the gun lock through a solenoid valve, situated outside the vacuum vessel and opened for about 10 ms. In front of the valve hydrogen gas, which is used as propellant, has an adjustable pressure of 5 to 40 bar and tempe-

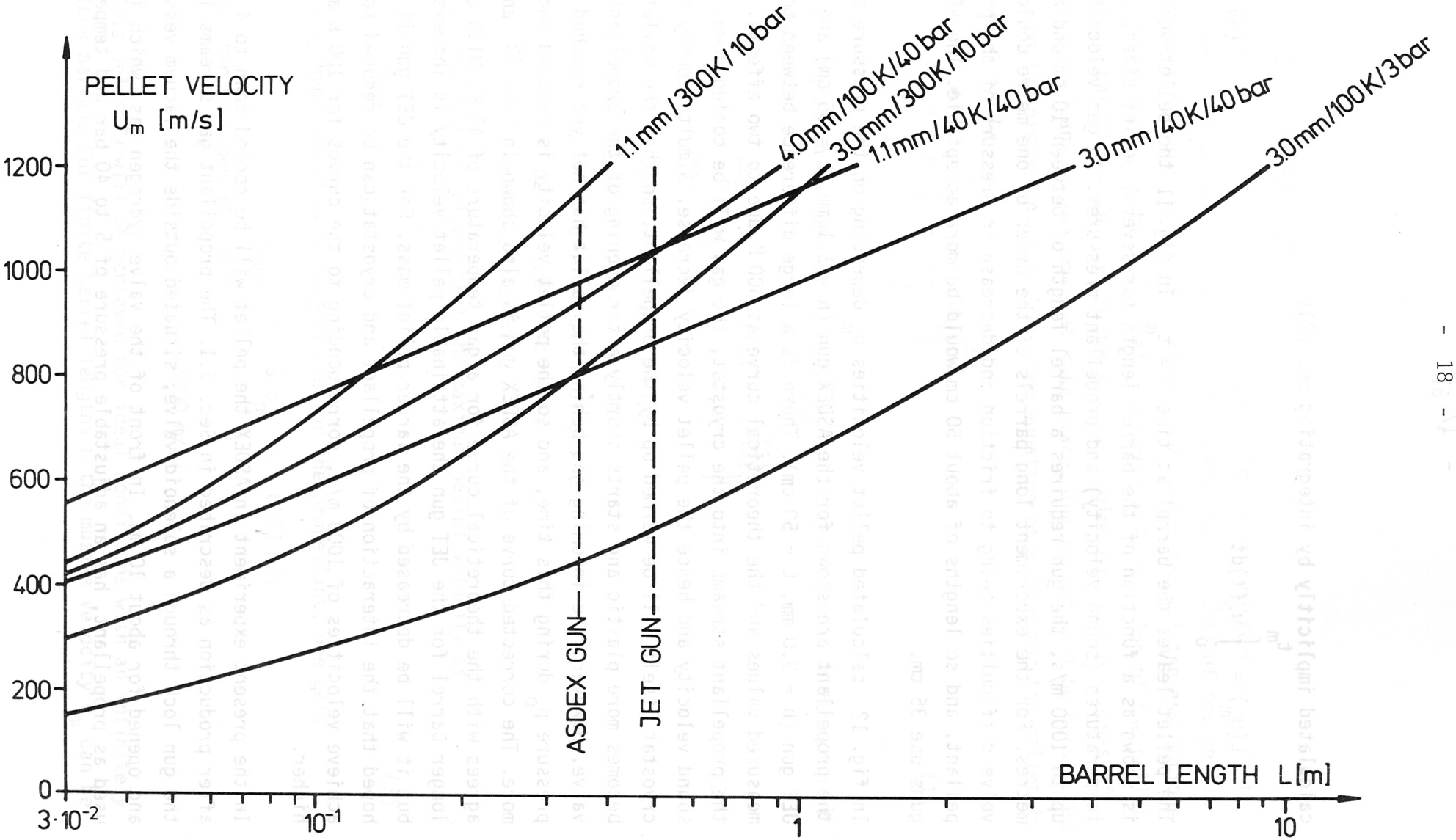

Fig.11 Pellet velocity versa barrel length for different pellet sizes, propellant temperatures and propellant pressures

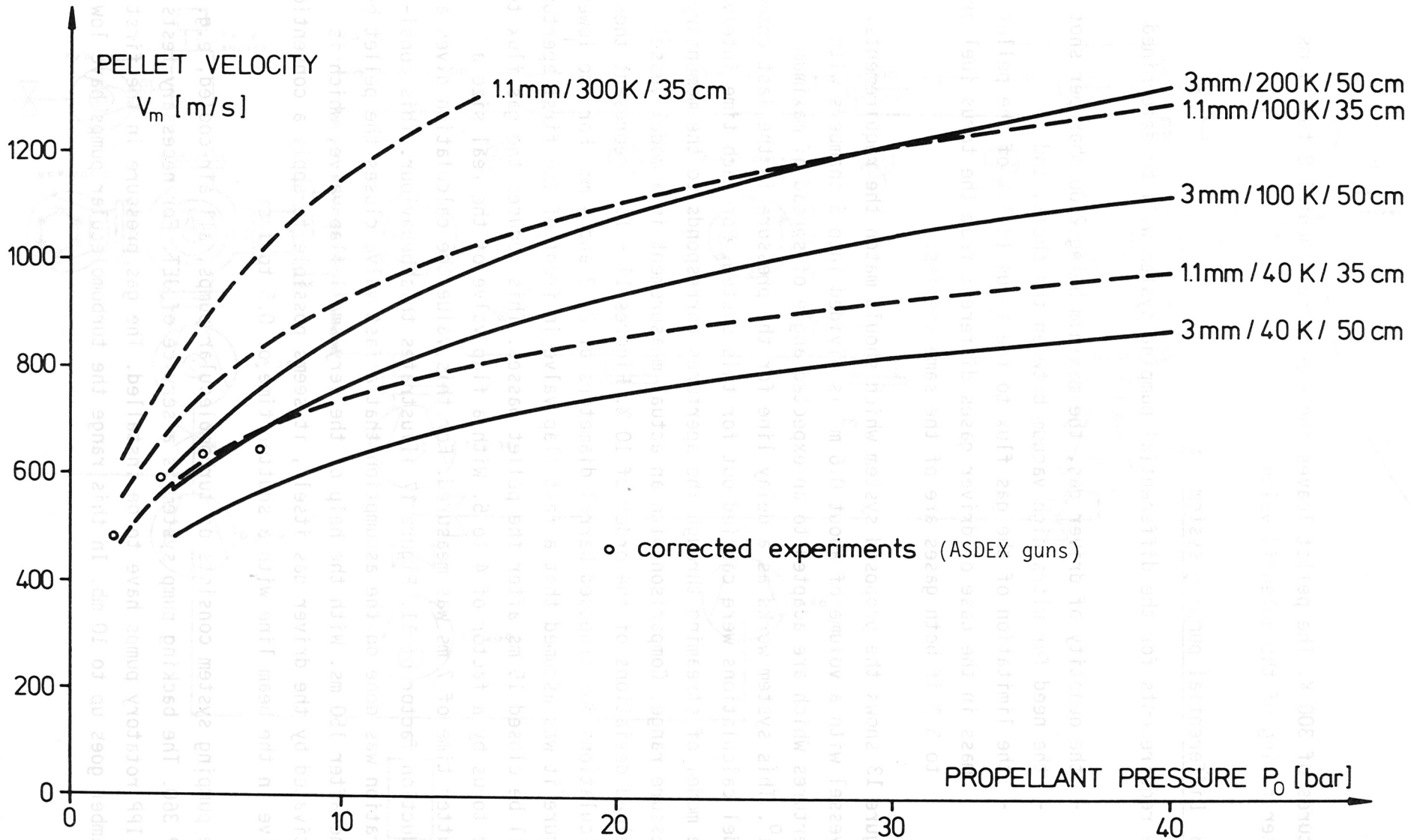

Fig.12 Pellet velocity versa propellant pressure for different pellet sizes, propellant temperatures and barrel lengths

ratures of 300 K. The pellet leaves the gun barrel about 1.8 to 2.1 ms after firing of the solenoid valve.

3.3 Differential pumping system

The requirements for the differential pumping system will be determined by

- the quantity of driver gas, the maximum being 2500 mbar per shot
- the need for ultra-high vacuum between the shots, and
- the limitation of the gas flux to the torus to 1 % of the pellet mass in the case of driver gases different from the torus fuel or to 5 % if both gases are of the same species.

Figure 13 shows the proposed system which should match the requirements. A vessel with a volume of about 0.6 m^3 is divided into 5 chambers with apertures which are adapted to an expected angle of spread of maximum $\pm 1^o$. This system works as a delay line for the pressure in the last chamber. Model calculations were carried out for this system. For each time interval the model of streaming through the apertures corresponds to the momentary pressure range. Comparison with an actual measurement in a model vessel yielded deviations of the order of 10 %. Figures 14 - 16 represent these calculations for proposed barrel diameters of 2, 3 and 4 mm. For the lower figure it was assumed that a fast flap valve in front of the first aperture will be closed 15 ms after the pellet passes. This reduces the gas flux to the torus by a factor of 4 to 5. With a flap valve of the real size a shutter time of 7 ms was measured. For this value the calculation gives a reduction factor of 11. Figure 17 illustrates this behaviour. This consideration was done on the assumption that a fast valve closes the pellet beam line after 150 ms. With the help of the very small flap valve, which is activated by the driver gas itself, it seems possible to apply a conventional valve in the beam line with a shutter time of 0.5 to 1 s.

The pumping system consists of turbomolecular pumps, all air-cooled, e.g. TVP 360. The backing pump system is a service of JET. For necessary tests at IPP rotatory pumps have to be installed. The gas pressure in the first chamber goes up to 10 mb. In this range the turbomolecular pumps have low

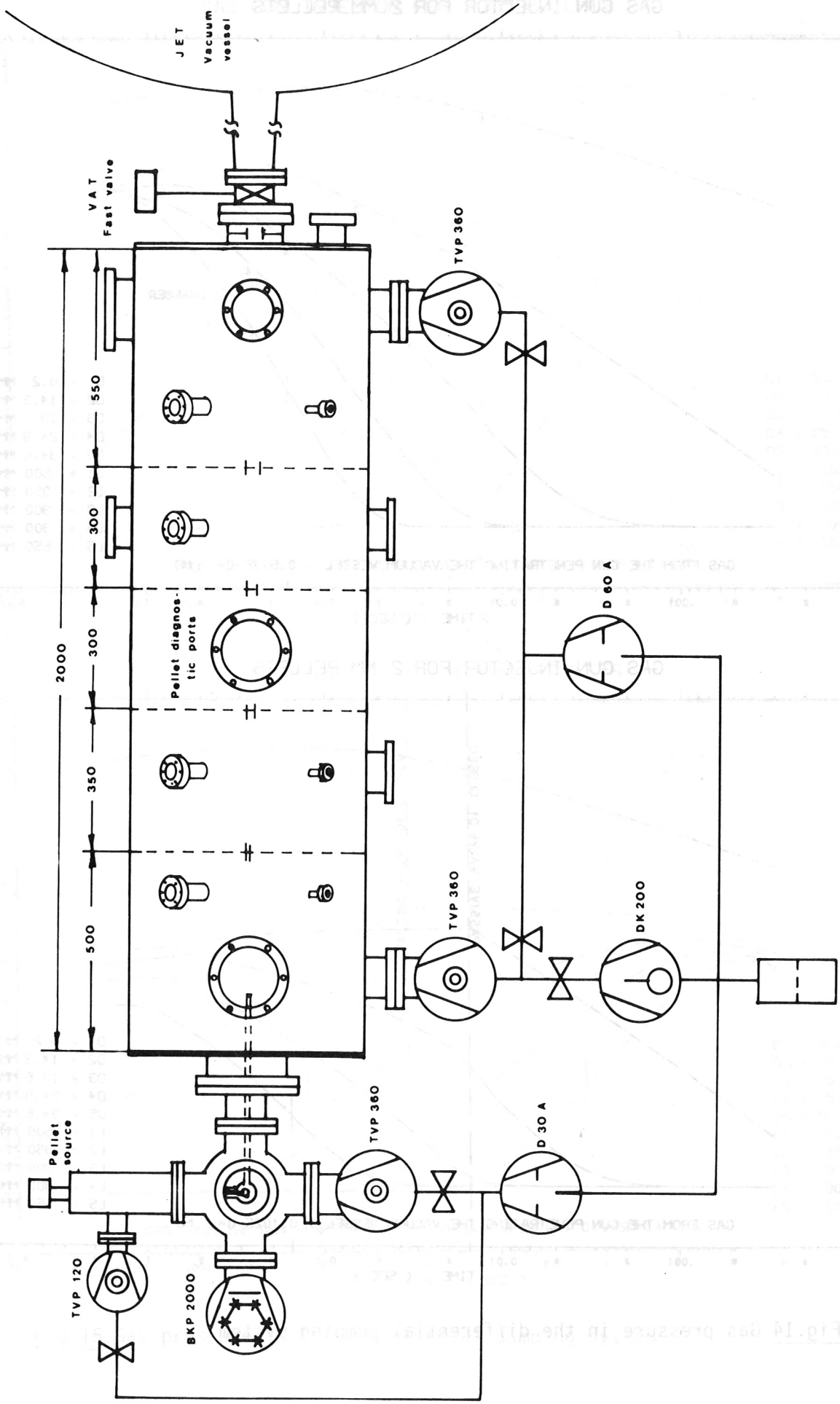

Fig.13 Differential pumping system for a pellet light-gas gun

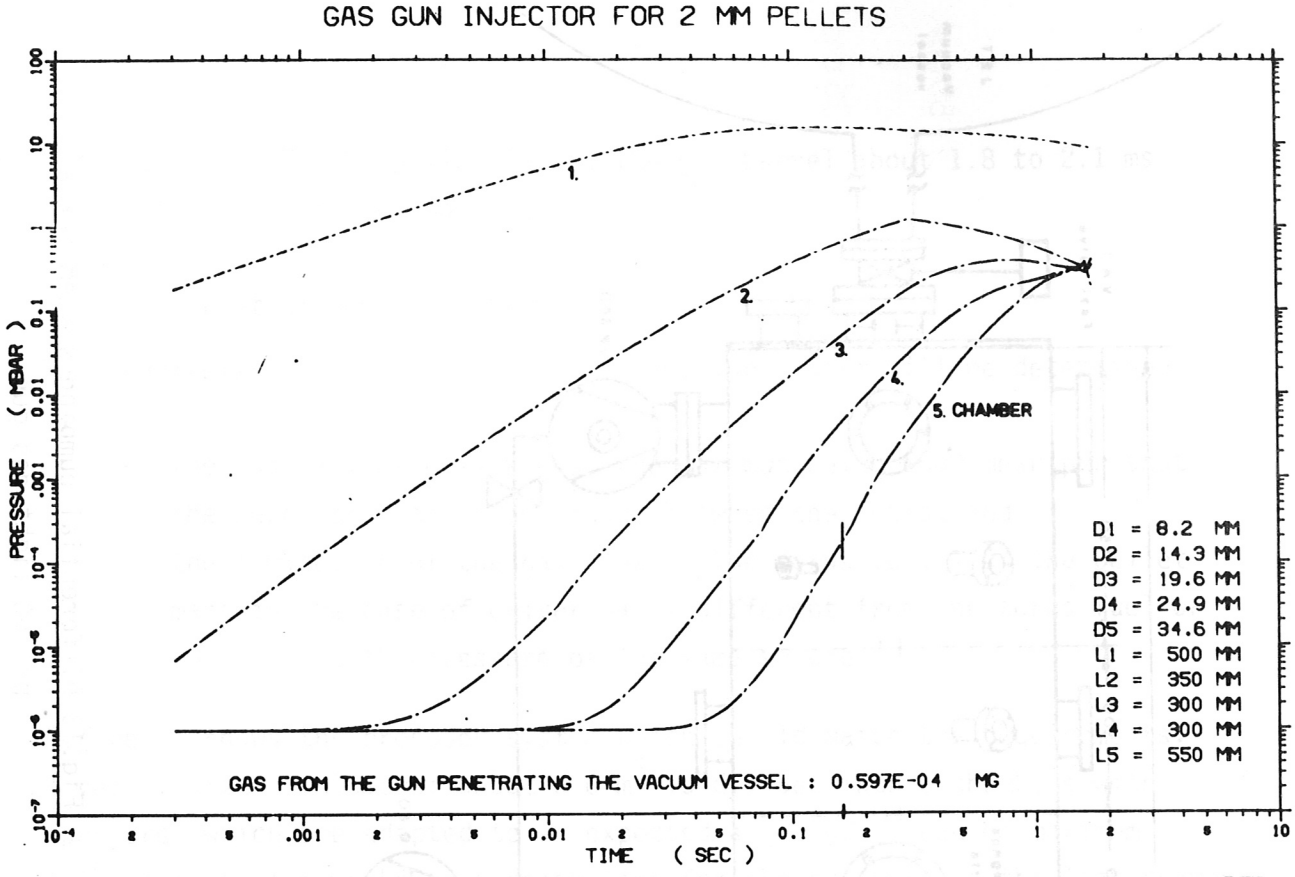

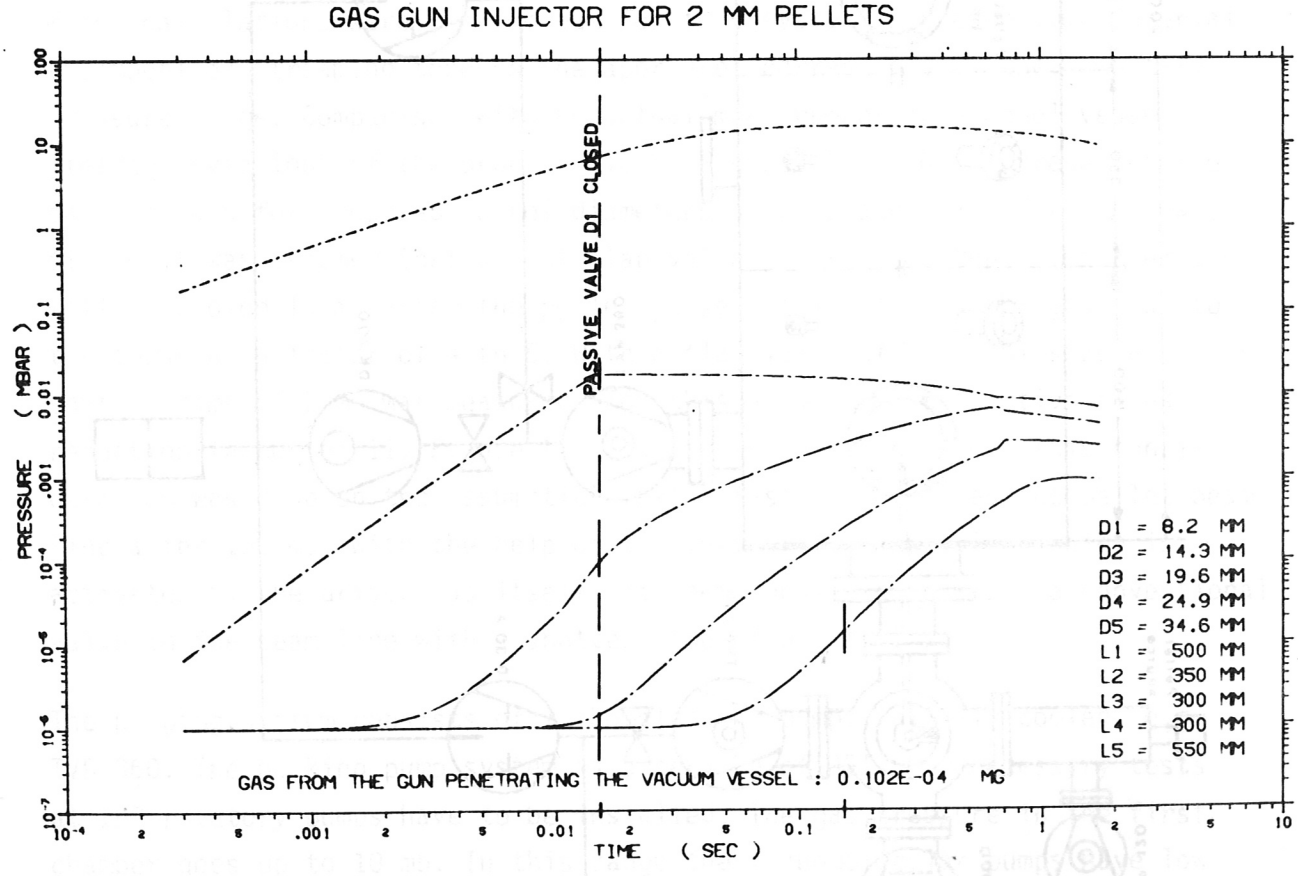

Fig.14 Gas pressure in the differential pumping system

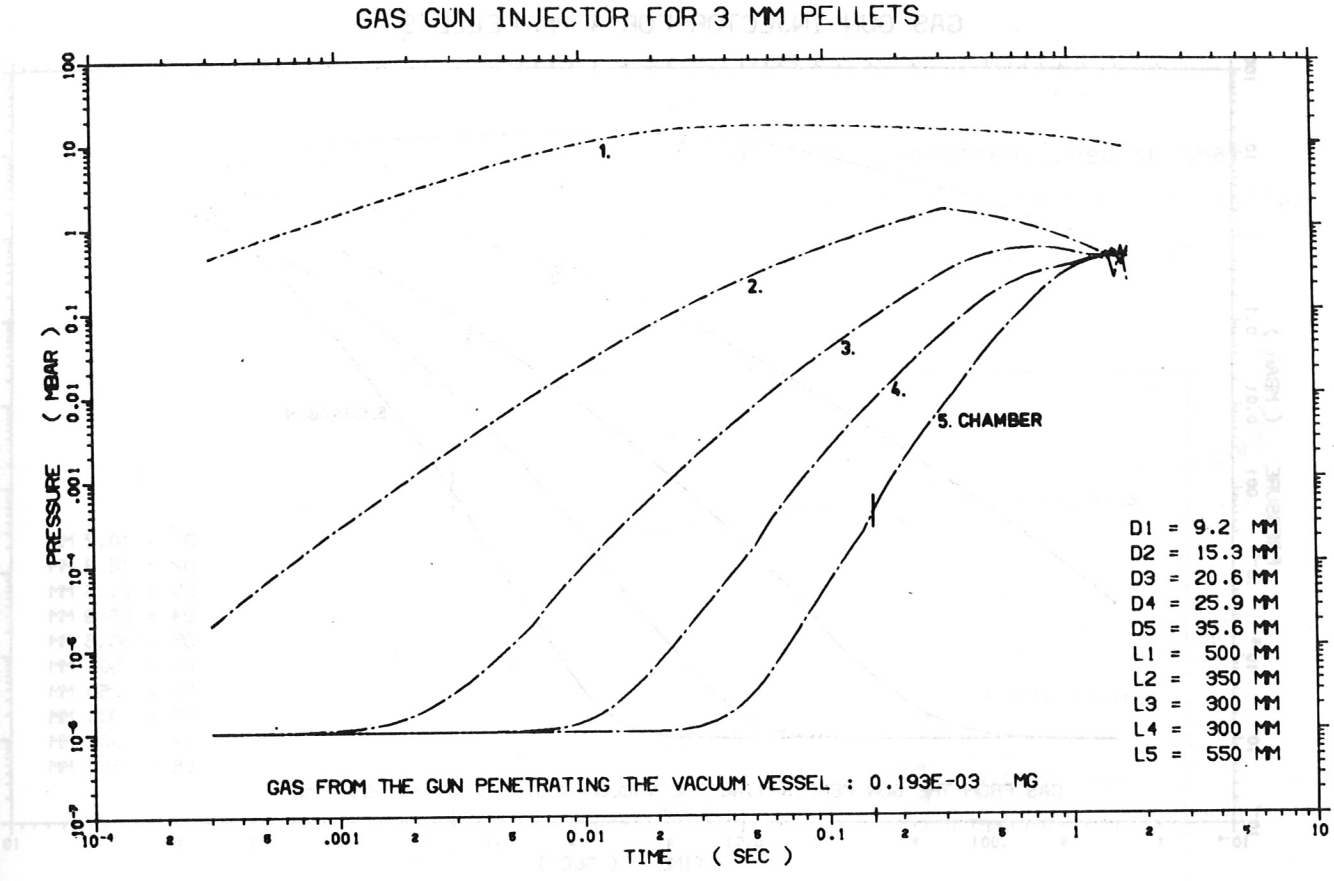

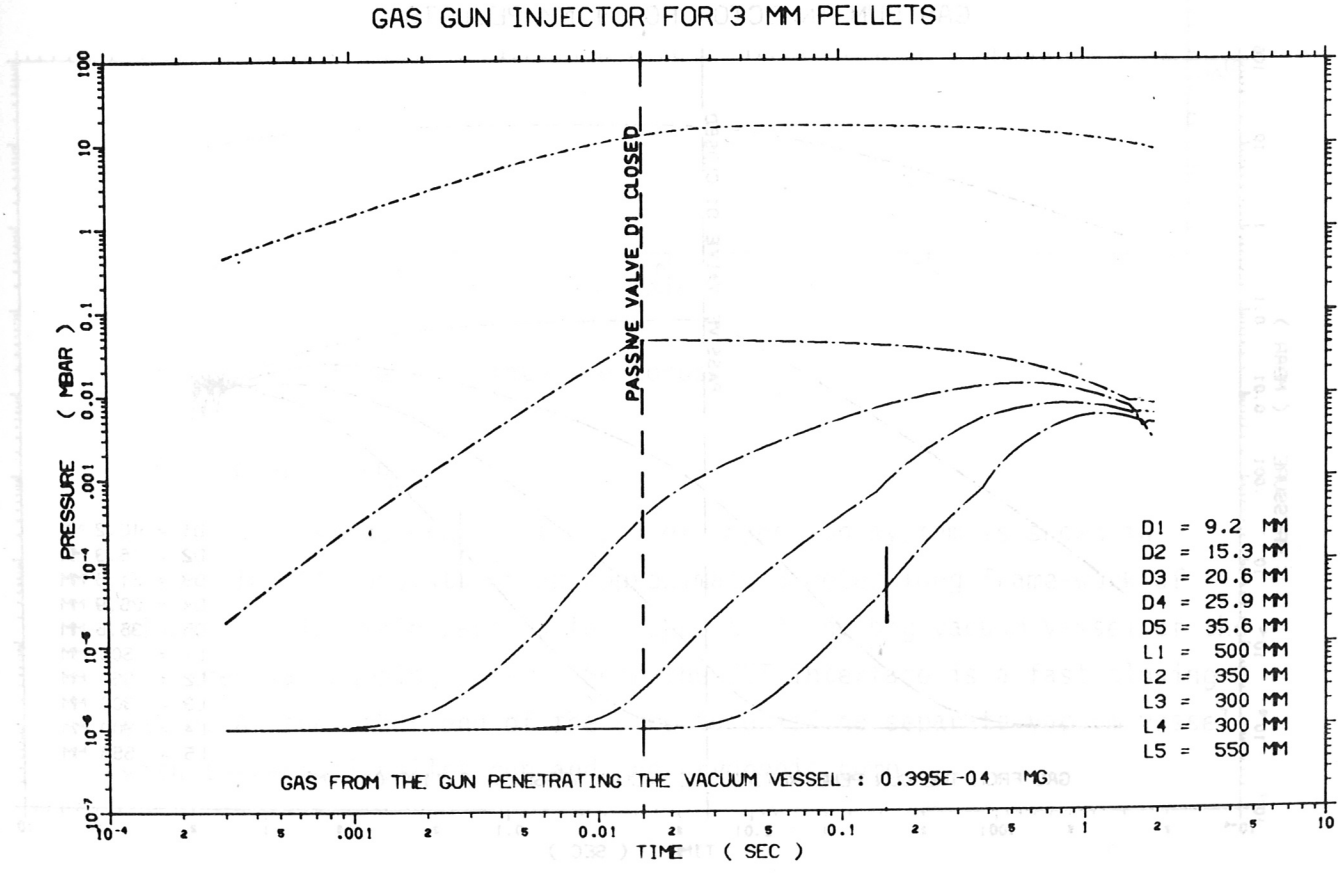

Fig.15 Gas pressure in the differential pumping system

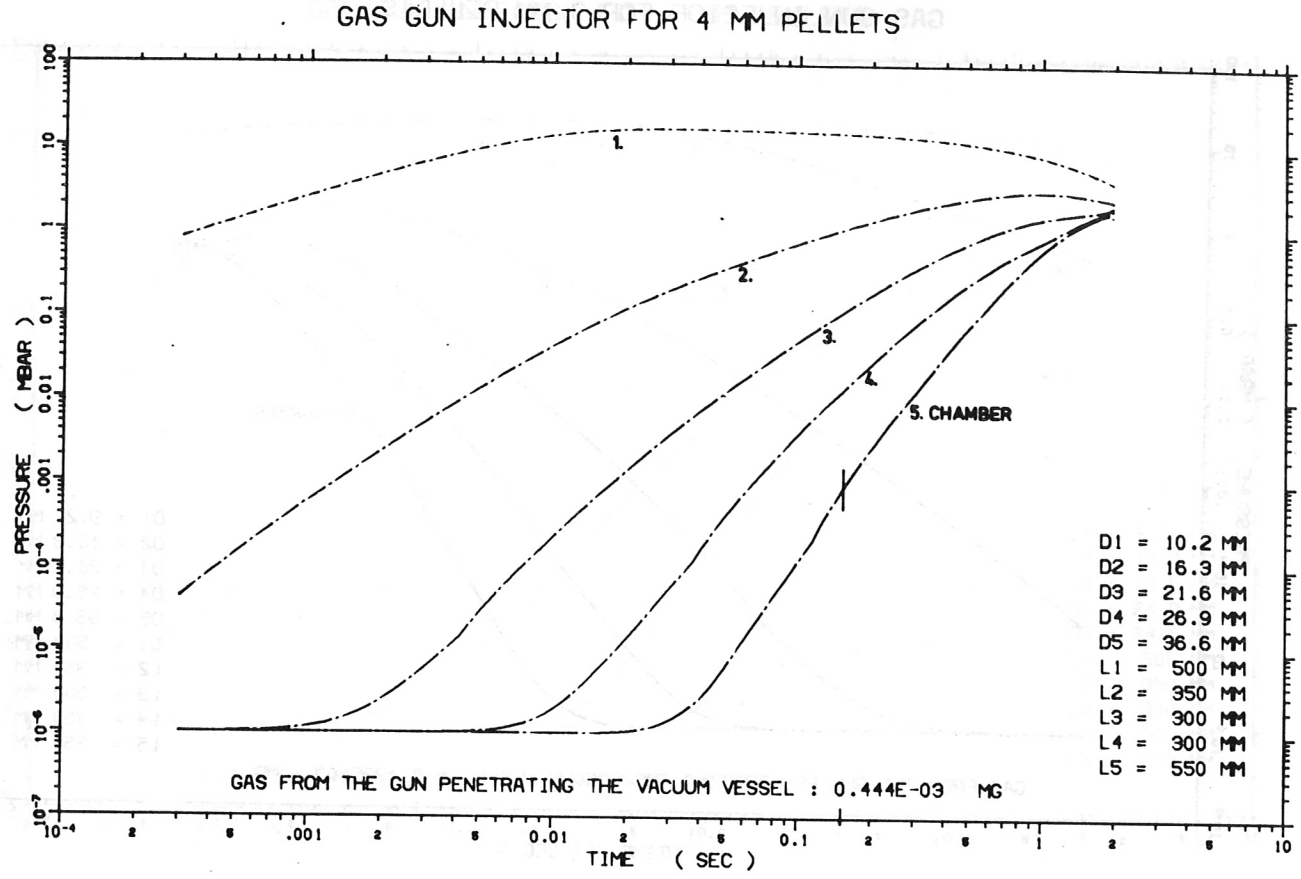

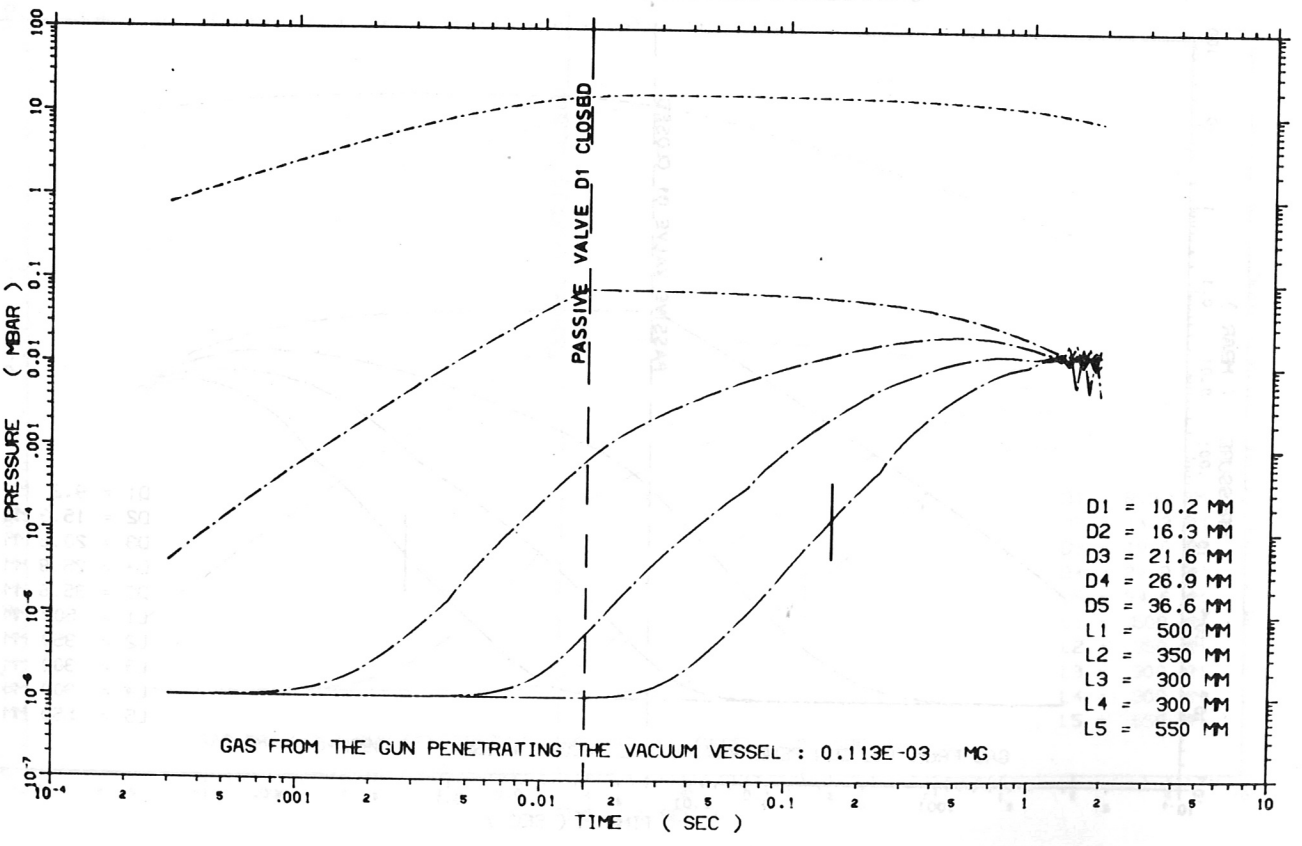

Fig.16 Gas pressure in the differential pumping system

efficiency. The rotary pump therefore has to be overdimensioned so that the pressure decreases to 10^{-3} mb in about one minute. After that a smaller pump (60 m^3/h) will be enough and the large one will be switched off.

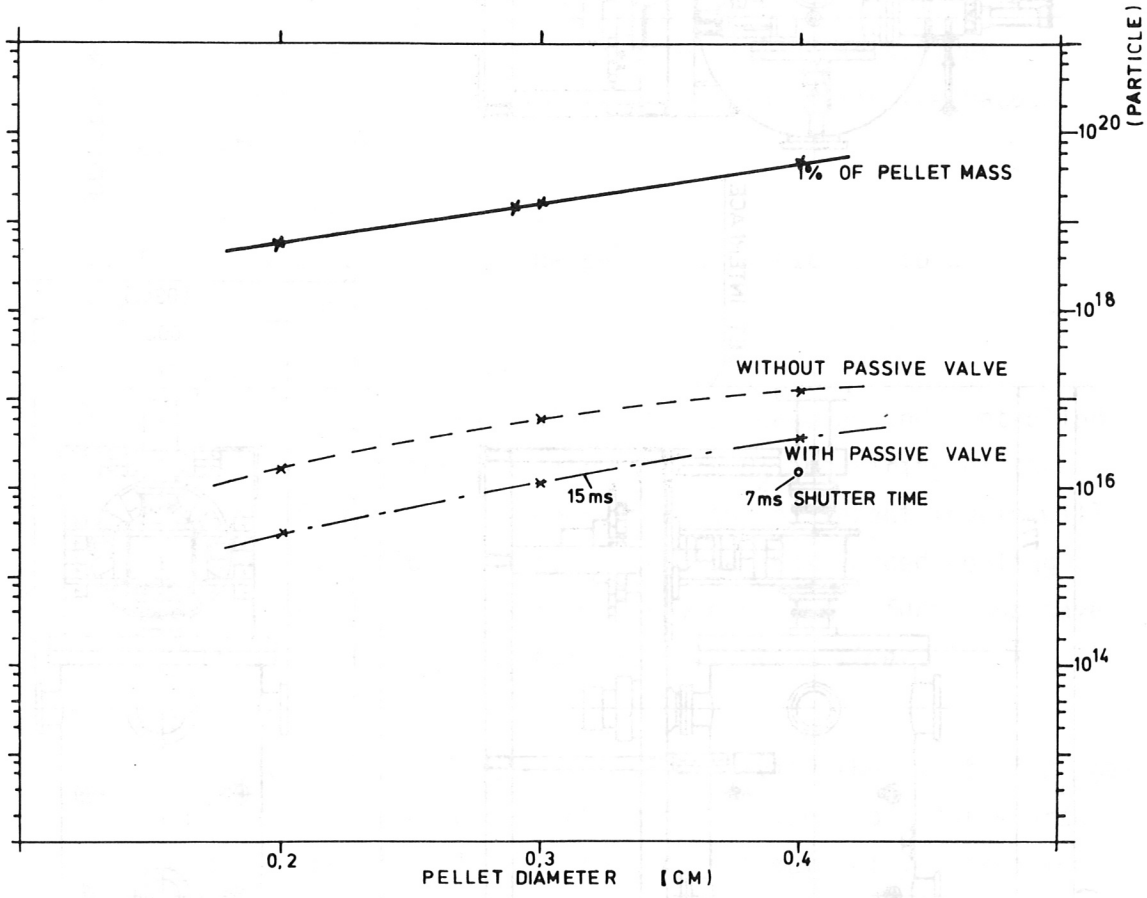

Fig. 17 particle flux into the torus

3.4 Support structure

The support structure for the pellet injection system is shown in figure 18. It consists of an approximate 3 meter long frame-work of aluminium. The main part is the support of the big vacuum vessel of the differential pumping system. Near the JET interface is a fast closing valve. At the other end of the structure is the separate vacuum vessel with the actual pellet gun and the cryogenic pump.

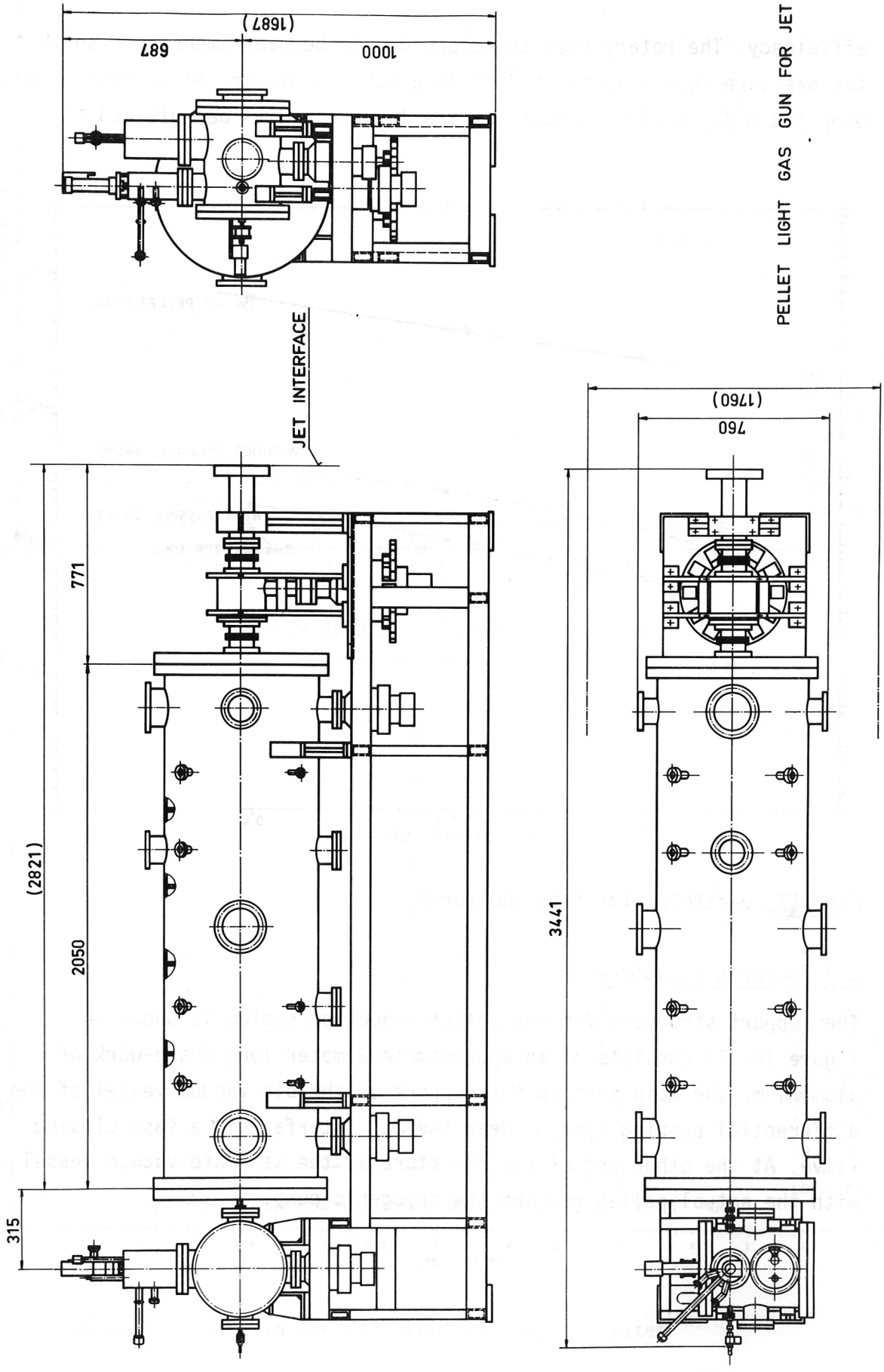

Fig.18 Total view of the pellet light-gas gun

3.5 Control system

The control system covers the following parts:

- Vacuum system
  It includes the control of pumps, valves, the vacuum measuring devices and the safety system, which in case of an accident switches the pumps off, closes the valves and fills the vacuum vessels with helium gas
- Flow of liquid helium
  The flow of the coolant for the pellet cryostat has to be automatically controlled
- Temperature control of cryostat
  The temperature of the cryostat has to be measured and controlled for solidification, storage, extrusion of D_2 and firing of the gun. Starting from a basic temperature, the different levels will be reached by electric heating. During the shot forced cooling by increased helium flow has to be provided. These functions have to be done both manually and automatically by a timer.
- D_2 supply
  During solidification of D_2 in the store cavity the inlet of D_2 gas has to be remotely controlled and measured. The amount of stored D_2 should also be directly recorded. An automatically controlled Pd filter unit for purification of D_2 will be included.
- Propellant gas
  Adjustment of the gas pressure should be possible from the control unit. The inlet valve of the propellant gas also has to be triggered from the control unit.
- Vacuum valves
  The principal purpose of the valves in the vacuum system along the pellet line is to prevent propagation of the propellant gas into the JET torus. The positions of the valves therefore have to be indicated in the control unit. They have to be opened before and closed shortly after the shot.

- Timer
  The pellet timer will be trigged by JET CODAS and then controls the time sequence for pellet production and injection as described in the last part of this section. The timer triggers the fire unit of the propellant valve and the pellet line valves.
- Cryopumps
  The content of liquid helium and nitrogen should be measured and the filling with coolants will be controlled automatically.

The interaction of the control unit with the pellet gun and the other systems is shown in fig. 19.

The control unit will be set up in the control room for JET, whereas the supplies to be controlled are positioned at or near the pellet gun.

One period of pellet production and injection is figured out in the diagram in fig. 20. It will be explained in the following.

The cryostat is controlled to have a basic temperature of about 8 K. The cycle starts with opening of the D_2 inlet valve and solidification of D_2 in the store cavity. After a time triggered by a signal from JET, the extrusion phase starts. A signal from the extruded D_2 stick stops extrusion by lowering the temperature followed by cutting and positioning the pellet in front of the barrel by rotation of the motor-driven gun lock. The pellet is then in waiting position, ready to fire. The command to fire is given by JET. This trigger will be delayed in the timer of the control unit to start some auxiliary systems. The pellet line valves and the cameras have to be opened, the pellet diagnostics have to be reset. If free-running diagnostics, e.g. solid-state cameras, are used, the trigger of the propellant valve should be synchronized with those devices. Immediately after the shot the pellet line valves are closed. The temperature will increase to the basic temperature. When all vacuum vessels have achieved their working pressures, the system starts the cycle again with condensation of D_2 and then waits again for the first JET trigger signal to start pellet production. The control unit used for ASDEX has to be improved in some way, e.g. the temperature control, and the complete system thus has to have remote control.

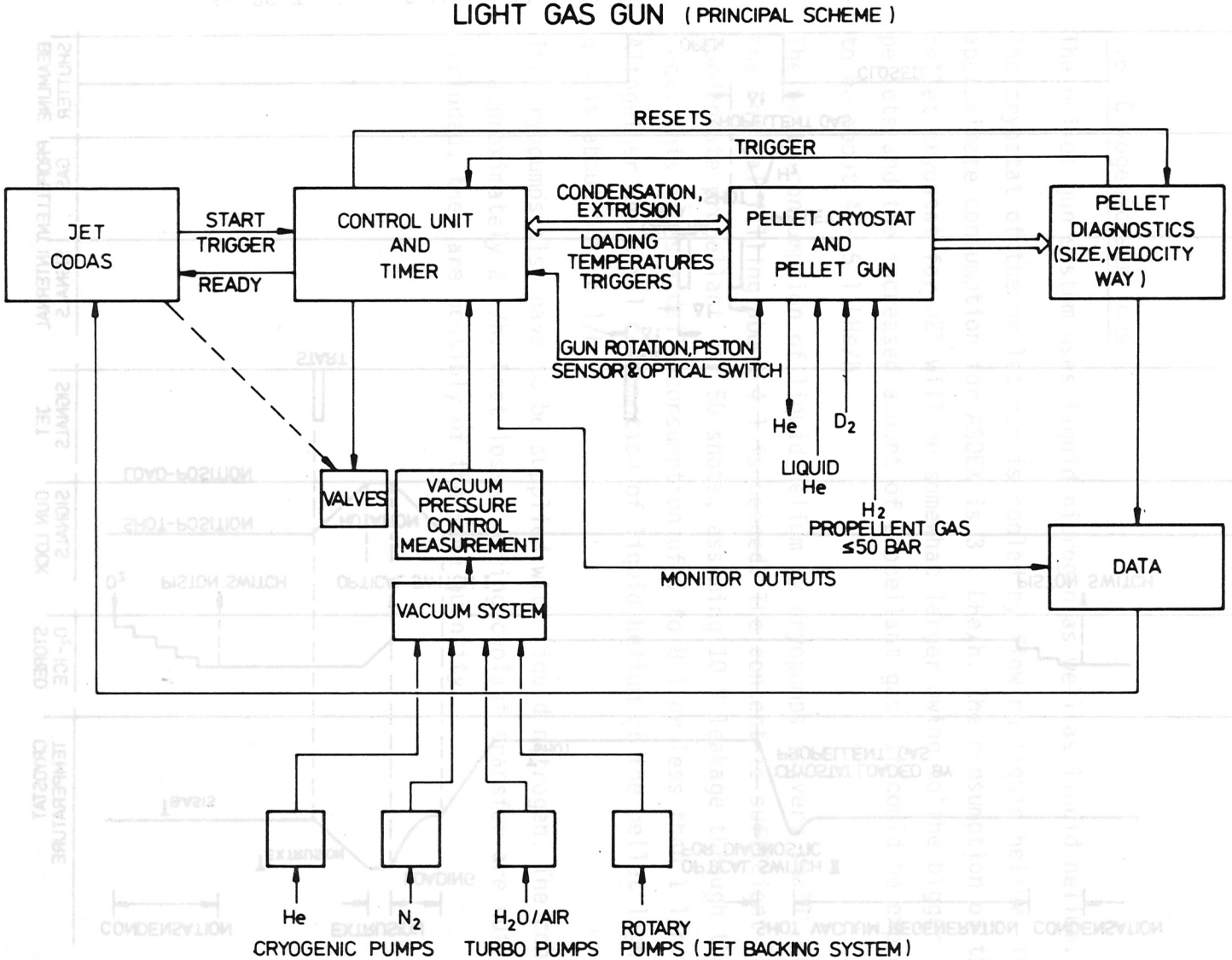

Fig.19 Pellet light-gas gun block diagram

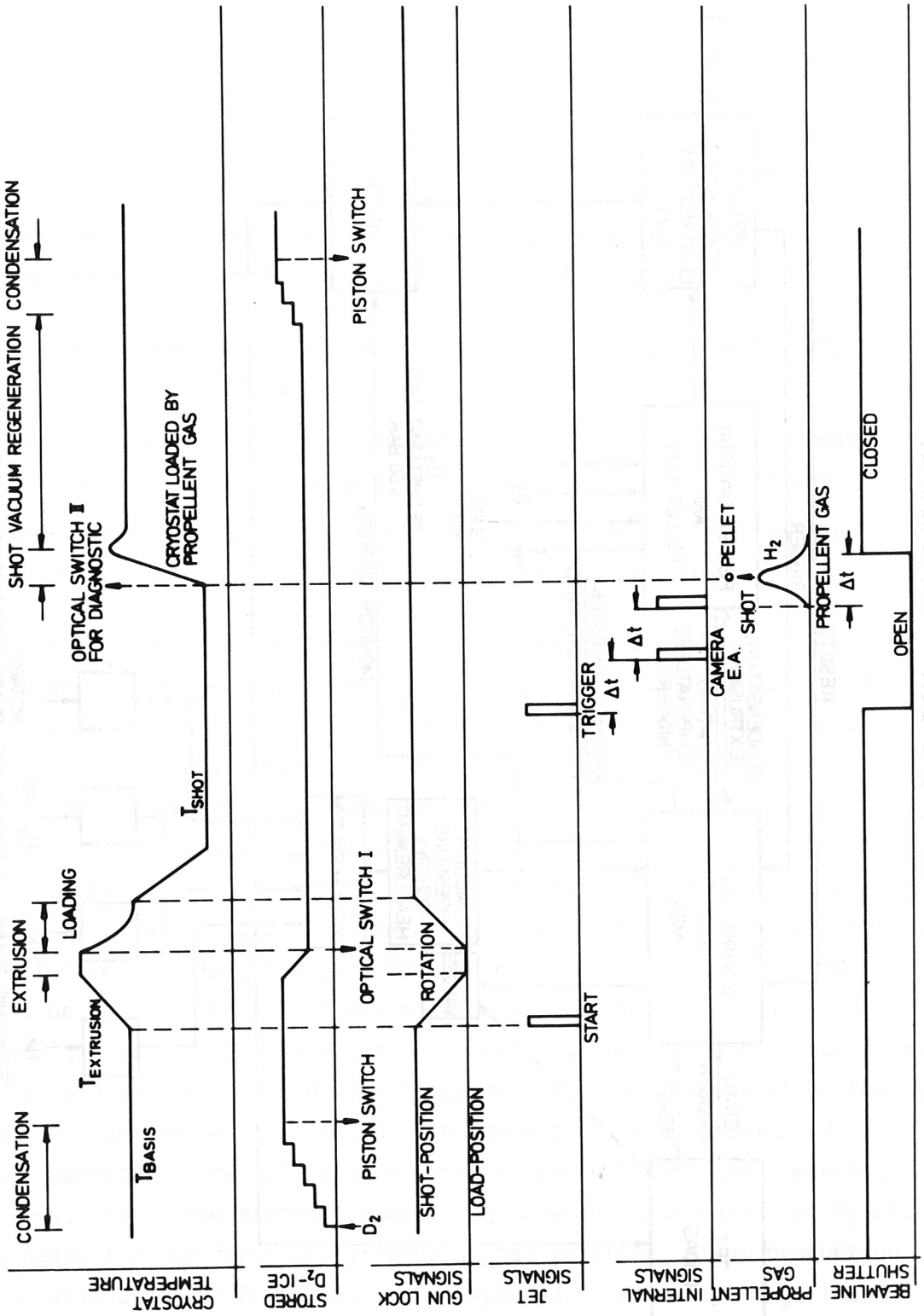

Fig.20 Timing of the pellet light-gas gun

The solid-state electronics used will certainly be sensitive to the high X-ray and neutron fluxes near the experiment. It has to be replaced by non-sensitive devices, or lightguide systems should be used and the sensitive elements will be protected by radiation shields.

3.6 Cryogenic services

The pellet gun system uses liquid nitrogen as well as liquid helium.

The cryostat of the pellet gun is cooled by flowing liquid helium. The approximate consumption for ASDEX is 3 l LHe/h. The consumption of the pellet cryostat for JET will be somewhat larger owing to the bigger pellets and the increased amount of propellant gas. It could be expected to be about 4 - 5 l LHe/h.

The basic consumption of liquid helium by cryopumps is very small. For the initial filling about 4 l is needed. The content is sufficient to condensate propellant for 50 shots, assuming 10 % leakage through the gun lock. This means a daily consumption of 6 to 8 l or less than 1 l/h. Altogether the total consumption of liquid helium of the pellet light-gas gun is about 5 to 6 l/h.

The cryopumps also have to be supplied with liquid nitrogen. The consumption is approximately 2 l/h. Heat losses during coolant transfer are not included, they are possibly of the same quantity.

4. Centrifuge Pellet Injector /8, 9, 10/

The centrifuge injector is thought as a tool for quasistationary refuelling in cases where the recycling is smaller than one. Before getting real experimental experience with JET discharges, it is difficult to determine the required pellet size and frequency. The pellet size will be mainly determined by the deposition profile wanted, the frequency by the particle confinement time and pellet size. Experience with ASDEX discharges has shown refuelling with pellets containing 20 to 40 % of the total particle complement is desirable. For a particle replacement time of about one second the pellet frequency is of the order of a few hertz. To be prepared for shorter replacement times, we envisage an upper frequency of 30 Hz.

The final pellet size should be determined after experimental results with the gas gun injector. The centrifuge injector itself will be able to handle pellets with diameters of 2 to 4 mm if some parts in the deuterium cryostats can be replaced.

4.1 Pellet production and feed-in

Pellet production will be done with the approved pellet source of Leybold-Heraeus as described for the light gas gun. This pellet source has a storage volume of 750 mm^3.

pellet size	2 Ø × 3	3 Ø × 3	4 Ø × 3 mm
volume	9.4	21.2	37.7 mm^3
pellet number	65	30	15

A larger storage volume requires further development of the cryostat but a factor of about four seems feasible.

The major problem and uncertainties stem from the method of feed-in into the centrifuge. The revolution time of the centrifuge will be 2 ms. Within this time the pellet must be transported a little more than its own length, corresponding to velocities of about 2 m/s. In principle, there are two methods of doing this if the pellet frequency is to be a free parameter. A deuterium ice rod will be produced by slow extrusion and stored in a second cryostat combined with the extrusion cryostat /11/ (see Fig.21). The

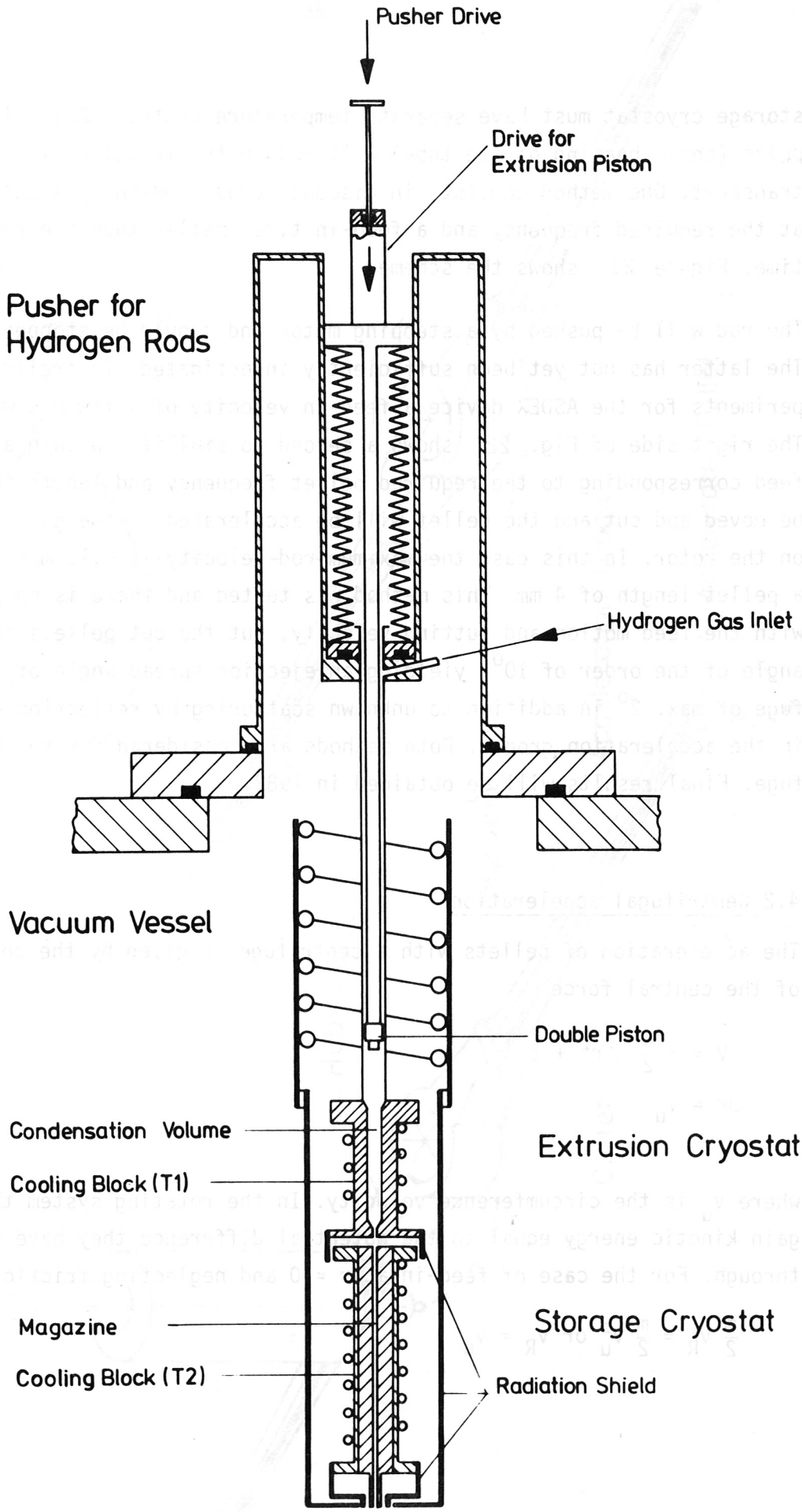

Fig.21 Cryostat for solid deuterium rod production

storage cryostat must have separate temperature control. A small heat pulse (ohmic heating of the tube) will reduce the friction of rest for fast transport. One method consists in discontinuous feed-in by a pellet length at the required frequency and a feed-in time smaller than the revolution time. Figure 22 shows the scheme.

The rod will be pushed by a stepping motor and should be stopped by friction. The latter has not yet been sufficiently investigated. In preliminary experiments for the ASDEX device a feed-in velocity of a few m/s was measured. The right side of Fig. 22 shows a second possibility. Within a continuous feed corresponding to the required pellet frequency and length the rod will be moved and cut and the pellet will be accelerated to the guiding groove on the rotor. In this case the maximum rod velocity is 0.12 m/s for 30 Hz and a pellet length of 4 mm. This method was tested and there is no problem with the feed motion and cutting velocity, but the cut pellets have a spread angle of the order of 10^{o}, yielding an ejection spread angle of the centrifuge of max. 2^{o} in addition to unknown scattering by reflection and friction in the acceleration groove. Both methods are considered for the ASDEX centrifuge. Final results will be obtained in 1982.

4.2 Centrifugal acceleration

The acceleration of pellets with a centrifuge is given by the potential of the central force

$$V = -\frac{m}{2}\omega^2 r^2 + c$$

$$\omega r = v_u$$

where v_u is the circumference velocity. In the rotating system the pellets gain kinetic energy equal to the potential difference they have passed through. For the case of feed-in at r = 0 and neglecting friction one gets

$$\frac{m}{2} v_R^2 = \frac{m}{2} v_u^2 \text{ or } v_R = v_u$$

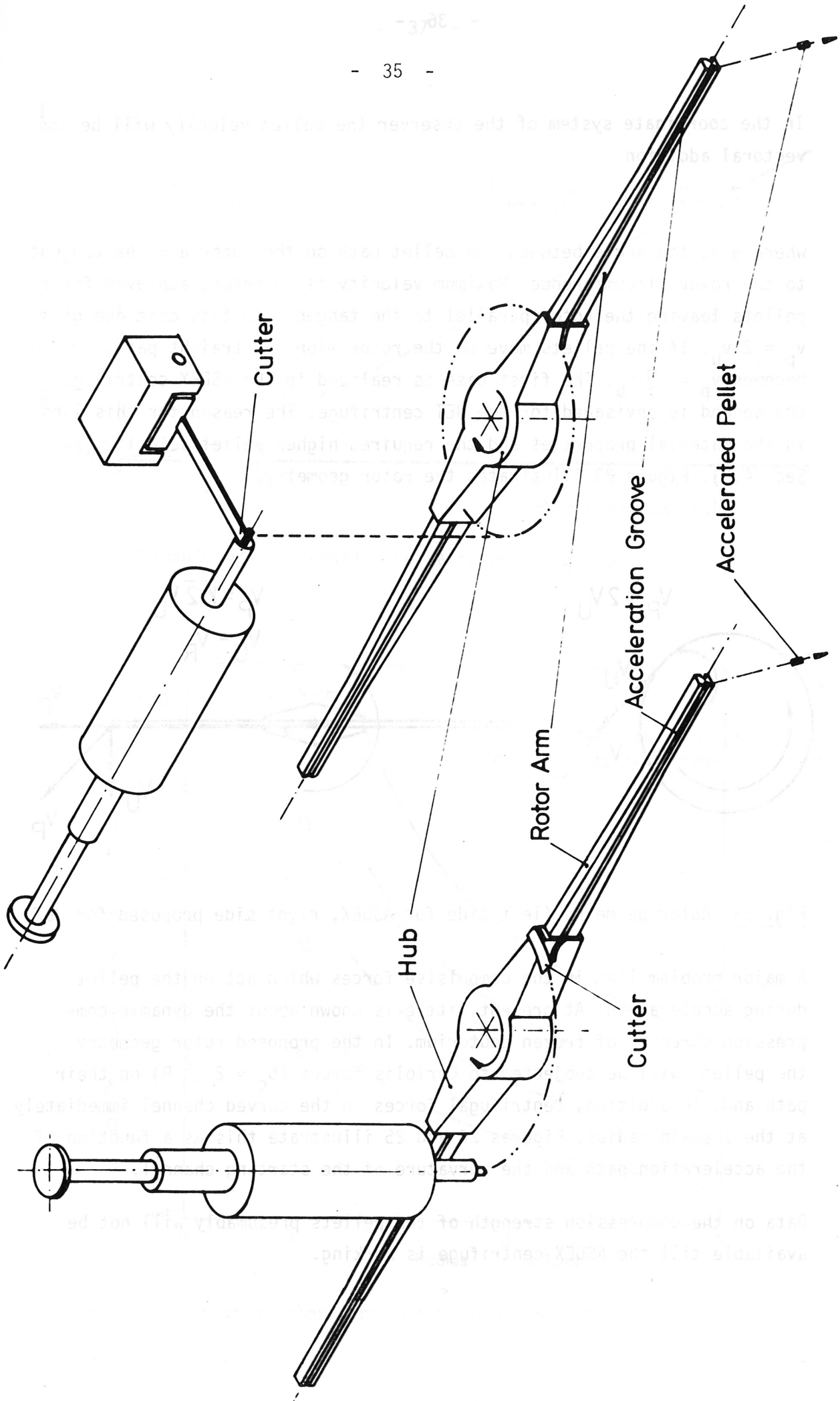

Fig.22 Methods of pellet feed-in

In the coordinate system of the observer the pellet velocity will be the vectoral addition

$$\vec{v}_p = \vec{v}_u + \vec{v}_R = 2v_u \cos \frac{\theta}{2}$$

where θ is the angle between the pellet path on the rotor and the tangent to the rotor circumference. Maximum velocity is therefore achieved for pellets leaving the rotor parallel to the tangent. In this case one gets $v_p = 2\ v_u$. If the pellets move on the rotor along a straight path, this becomes $v_p = \sqrt{2}\ v_u$. The first case is realized in the ASDEX centrifuge, the second is envisaged for the JET centrifuge. The reason for this lies in the material properties and the required higher pellet velocity (see Sec. 4.3). Figure 23 illustrates the rotor geometry.

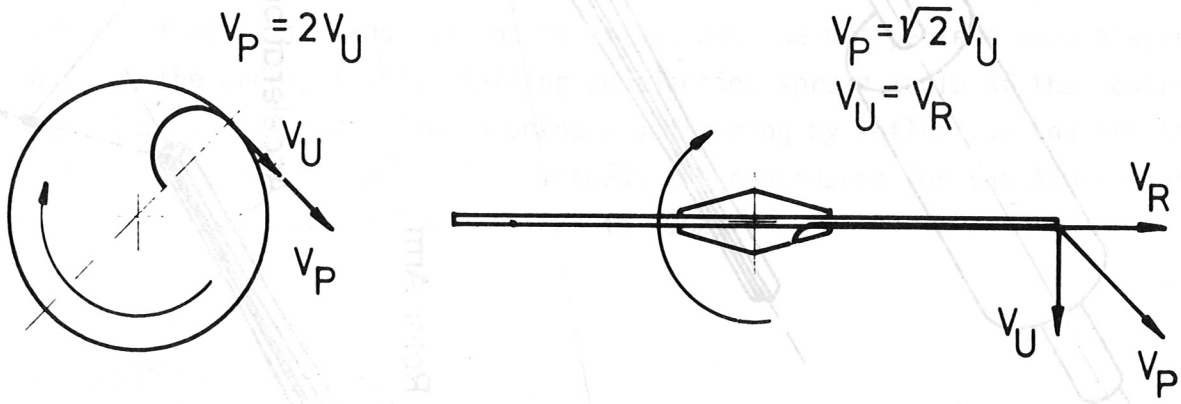

Fig. 23 Rotor geometry (left side for ASDEX, right side proposed for JET)

A major problem lies in the compulsive forces which act on the pellet during acceleration. At present little is known about the dynamic compression strength of frozen deuterium. In the proposed rotor geometry the pellets will be subjected to Coriolis forces ($b_c = 2\ \omega^2\ R$) on their path and, in addition, centrifugal forces in the curved channel immediately at the feed-in radius. Figures 24 and 25 illustrate this as a function of the acceleration path and the curvature of the starting channel.

Data on the compression strength of the pellets presumably will not be available till the ASDEX centrifuge is working.

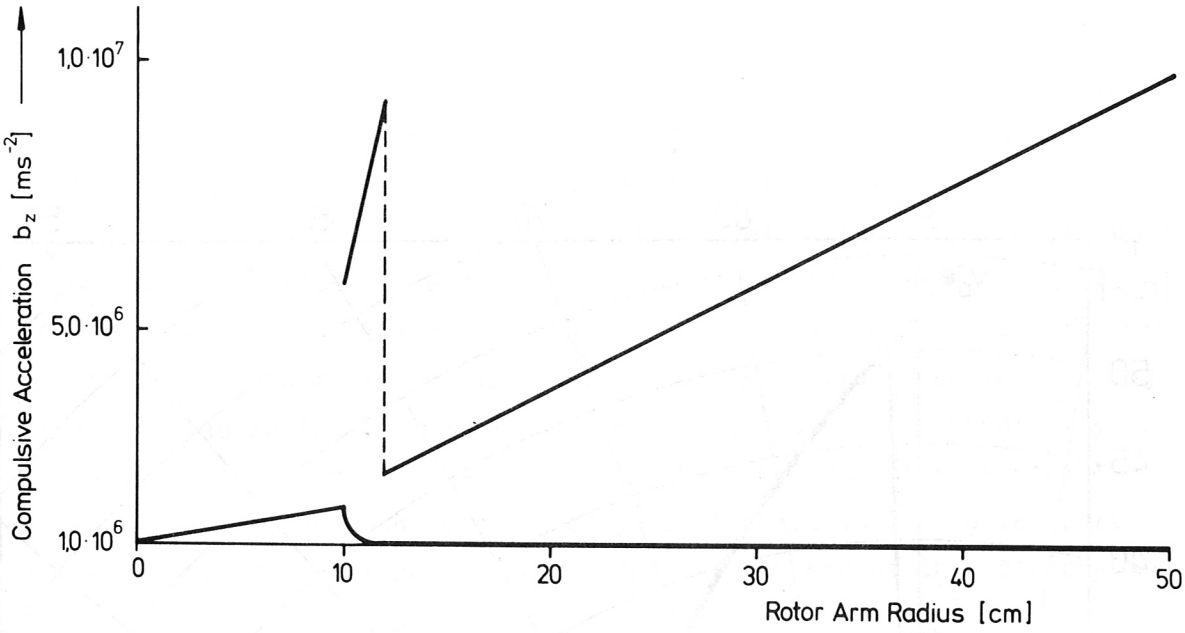

Fig.24 Compulsive acceleration versa rotor arm radius

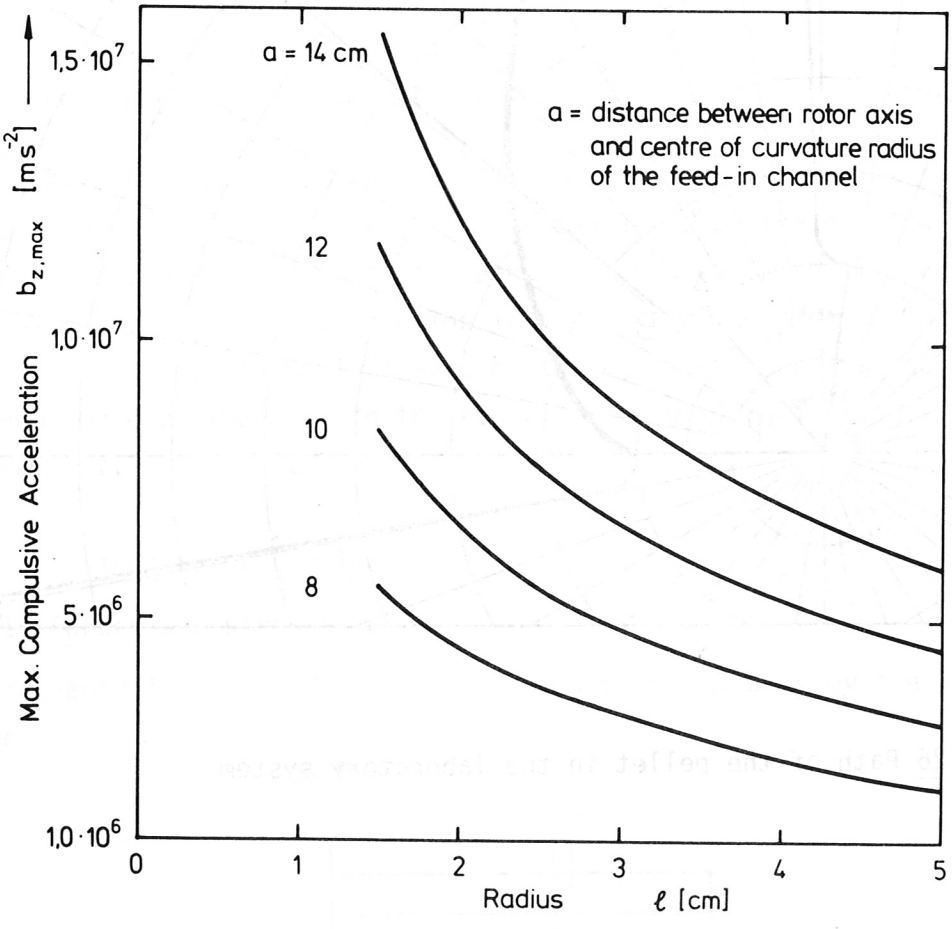

Fig.25 Compulsive acceleration versa curvature radius

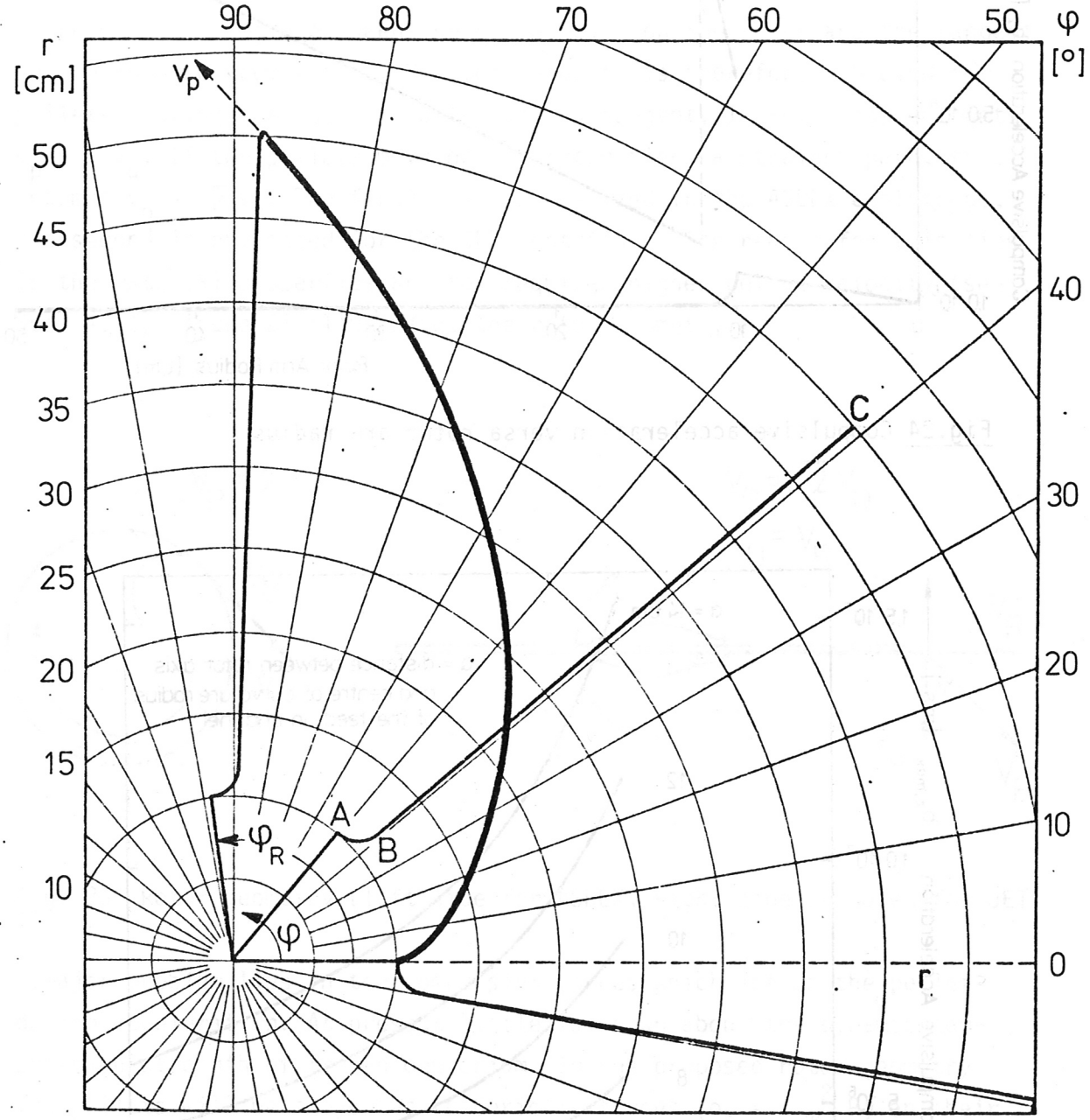

Fig.26 Path of the pellet in the laboratory system

More is known about the collision velocity which the pellets can survive. In centrifuge experiments with a straight guiding path we found a collision velocity of at least 54 m/s for pellet temperatures of about 7 K. From this value we deduct an allowable collision angle of about 10^{o} for a rotation frequency of 500 Hz and feed-in radius of 0.1 m. This has to be kept in mind for the mechanism of the pellet feed-in with regard to the spread angle. The pellet has to be introduced as tangentially as possible to the acceleration groove. In the proposed rotor version the curvature is chosen such that the compulsive force in the curved part of the groove does not become larger than at the end of the acceleration path.

Figure 26 shows the path line of the pellets on the rotor depending on the rotor angle. For the proposed values:

rotor radius	$R = 0.45$ m
feed-in radius	$r = 0.10$ m
curvature radius	$l = 0.02$ m
frequency	$\omega = 3142\ s^{-1}$.

The acceleration angle φ_R will be about 92^{o}.
A really open question is still the spread angle of the ejected pellets. Besides the feed-in process it depends on the real path of the pellet, including reflections and friction in the guiding groove. At lower speeds (300 m/s) practically no influence on the ejection speed was observed. Forthcoming experiments with the ASDEX device will deliver a criterion for the velocity range up to 700 m/s.

4.3 Mechanical rotor problems

4.3.1 Forces and stresses

The mechanical stress of the rotor is given essentially by the centrifugal force

$$F = m\omega^2 \cdot r \ .$$

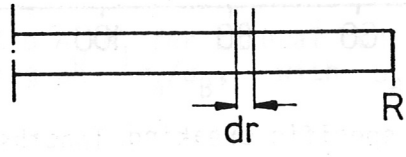

For a rotating rod with constant cross-section A we get

$$F(r) = A\rho\omega^2 \int_r^R r\,dr \qquad \text{or} \qquad F_{R_1} = A\rho\omega^2 \frac{R^2 - R_1^2}{2}$$

for the tensile stress at a radius R_1

$$\sigma_{R_1} = \frac{\rho\omega^2}{2} (R^2 - R_1^2)$$

The maximum tensile stress will be found at the rotation axis

$$\sigma_{axis} = \frac{\rho\omega^2}{2} R^2 \triangleq \frac{\rho}{2} v_u^2$$

with $v_u = \omega R$.

With reference to the pellet velocity after acceleration with a straight rod $v_p = \sqrt{2}\, v_u$ the maximum tensile stress will be

$$\sigma_{max} = \frac{\rho}{4} v_p^2$$

For comparison of different materials we looked for the specific breaking length σ/γ , with $\gamma = \rho \cdot g$

$$\frac{\sigma}{\gamma} = v_p^2/4g$$

For the planned pellet velocity of v_p = 2000 m/s and constant cross-section of the rotor arm the breaking length is 10^5 m. Figure 27 represents these values for several construction materials with high tensile strength.

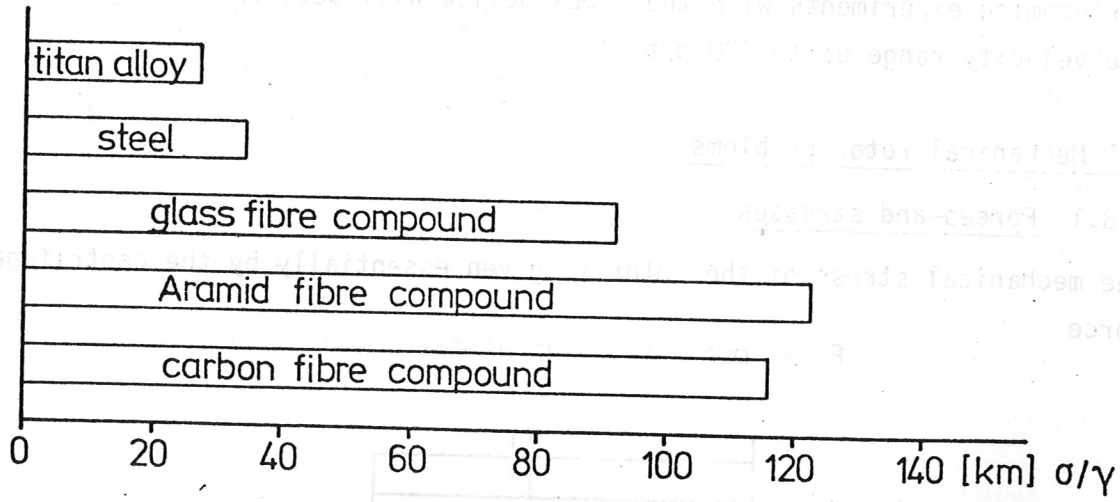

Fig. 27 Comparison of specific breaking lengths.

Only aramid and carbon fibre compounds show values greater than 10^5 m. Even with these materials the attainable safety factor is only somewhat over one. Tests carried out by MAN, Neue Technologien, with carbon fibre compound rods confirmed this behaviour.

The solution will be to fabricate a rotor rod with optimized cross-section. This means the cross-section increases with decreasing radius such that the tensile stress will be constant corresponding to the permissible tensile strength. The outer part will be a straight rod with constant cross-section down to a radius where the permissible tensile strength σ_a will be reached.

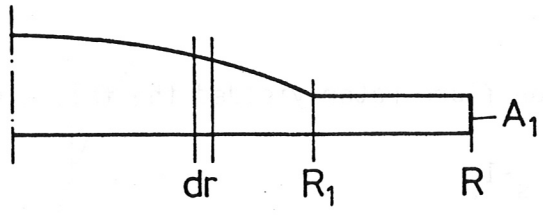

The solution for this condition delivers the necessary cross-section:

$$A(r) = A_1 \exp\left[\frac{\rho\omega^2}{2\sigma_a}(R_1^2 - r^2)\right] \text{ with } R_1 = \sqrt{R^2 - \frac{2\sigma_a}{\rho\omega^2}}$$

A comparison of A_o/A_1 for different materials and safety factors is given in Table I for a pellet velocity v_p = 2000 m/s; R = 0.45 m; $\omega = 3.14 \times 10^3\ s^{-1}$.

			$\sigma_{\parallel a} = 0.5\ \sigma_B$		$\sigma_{\parallel a} = 0.66\ \sigma_B$		$\sigma_{\parallel a} = 0.8\ \sigma_B$	
material	g[g/cm³]	σ_B[N/mm²]	R_1[m]	A_o/A_1	R_1[m]	A_o/A_1	R_1[m]	A_o/A_1
Al-alloy	2.7	340	0.43	$3 \cdot 10^6$	0.431	$55 \cdot 10^3$	0.427	$7.6 \cdot 10^3$
Ti-alloy	4.45	1000	0.42	$27 \cdot 10^3$	0.415	293	0.408	97
steel	7.9	1400	0.43	$3 \cdot 10^4$	0.423	$1.8 \cdot 10^3$	0.417	428
glass fibre*	2.0	1800	0.33	3.3	0.285	1.95	0.238	1.47
carbon fibre*	1.55	1800	0.29	2.0	0.214	1.34	0.120	1.08
Aramid fibre*	1.35	1650	0.281	1.89	0.194	1.26	0.068	1.03

Table I Cross-section ratio A_o/A_1 for several construction materials and R_1 values depending on σ_a/σ_B, with σ_B the breaking strength.

Even in the case of optimized centrifuge rotor cross-sections only fibre compounds show practicable small values of A_1/A_o owing to the high breaking strength and small specific weight. The advantage of high $\sigma_{\parallel}$ of the unidirectional compound materials is connected with the disadvantage of small $\sigma_{\perp}$ and small modulus of shear G. The increasing tensile stress at smaller radii has to be transmitted to the increased cross-section via the shear strength. This requires a large ratio of $G/E_{\parallel}$ (modulus of shear / modulus of elasticity). Besides the above-mentioned tensile stresses we have to consider shear stresses in the case of oscillations of the rotor arm.

Finite element calculation for the carbon fibre rotor yielded the following resonance frequencies:
$f_1 = 150\ s^{-1}$, $f_2 = 260\ s^{-1}$ and $f_3 = 680\ s^{-1}$.

It is planned to keep the rotor idling at a frequency somewhat above f_2 during "stand-by" and increase speed to operating frequency for pellet injection only. This operation mode will considerably reduce tensile stress in the rotor arm during "stand-by". Furthermore, the dynamic stress amplitude is reduced. Considering carefully the material properties, aramid fibre and carbon fibre compounds are both suitable for application in the centrifuge. It is planned to run some tests with full-size rotors at operating frequencies and 15 % above and below for 8 hours each.

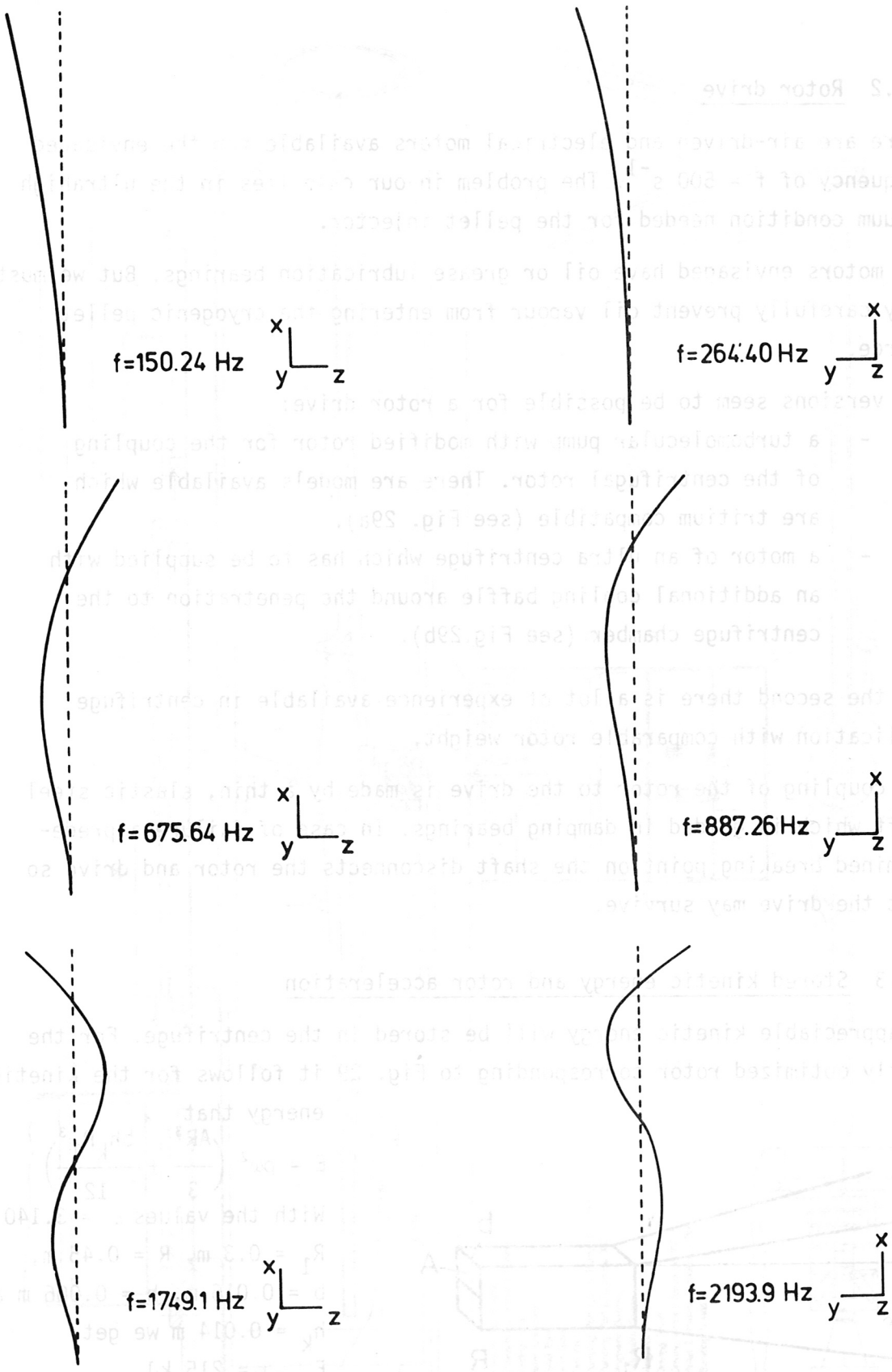

Fig.28 Oscillation modes for the optimized rotor arm

4.3.2 Rotor drive

There are air-driven and electrical motors available for the envisaged frequency of f = 500 s^{-1}. The problem in our case lies in the ultrahigh vacuum condition needed for the pellet injector.

All motors envisaged have oil or grease lubrication bearings. But we must very carefully prevent oil vapour from entering the cryogenic pellet source.

Two versions seem to be possible for a rotor drive:

- a turbomolecular pump with modified rotor for the coupling of the centrifugal rotor. There are models available which are tritium compatible (see Fig. 29a).
- a motor of an ultra centrifuge which has to be supplied with an additional cooling baffle around the penetration to the centrifuge chamber (see Fig.29b).

For the second there is a lot of experience available in centrifuge application with comparable rotor weight.

The coupling of the rotor to the drive is made by a thin, elastic steel shaft which is guided in damping bearings. In case of failure a predetermined breaking point on the shaft disconnects the rotor and drive so that the drive may survive.

4.3.3 Stored kinetic energy and rotor acceleration

An appreciable kinetic energy will be stored in the centrifuge. For the nearly optimized rotor corresponding to Fig. 29 it follows for the kinetic energy that

$$E = \rho\omega^2 \left(\frac{AR^3}{3} + \frac{bh_k R_1^3}{12}\right)$$

With the values ω = 3.140 s^{-1}, R_1 = 0.3 m, R = 0.45 m, b = 0.016 m, h = 0.006 m and h_k = 0.014 m we get

E_{rod} = 215 kJ.

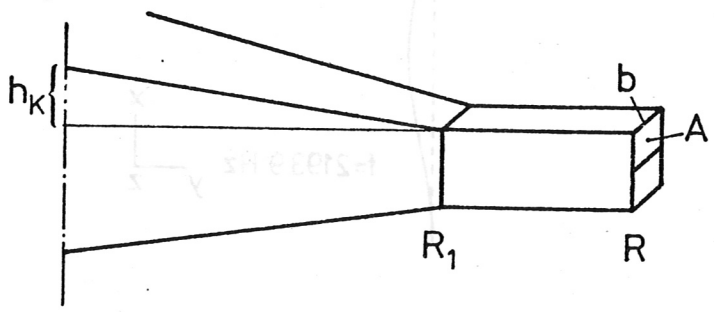

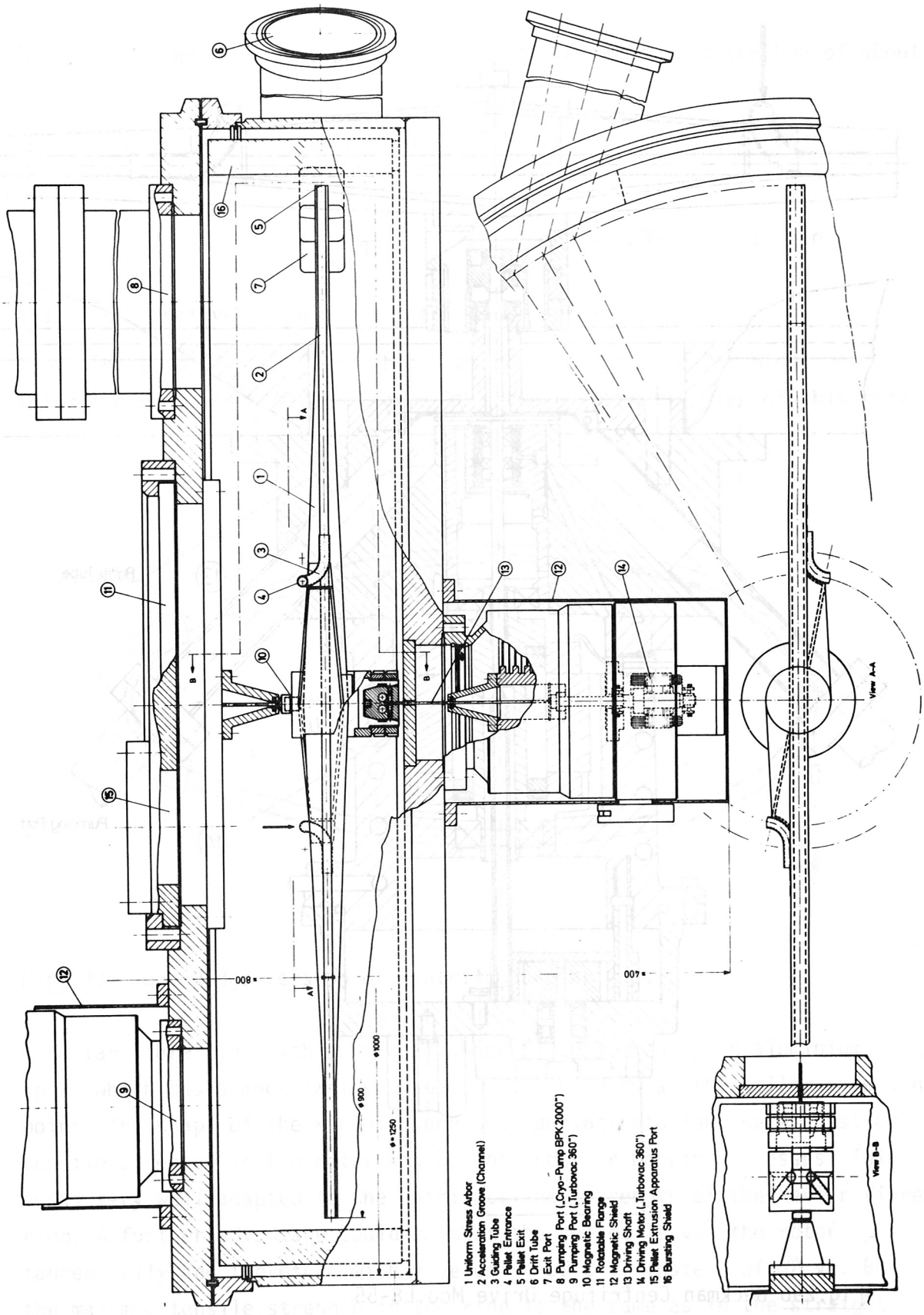

Fig.29a Centrifugal Pellet Injector

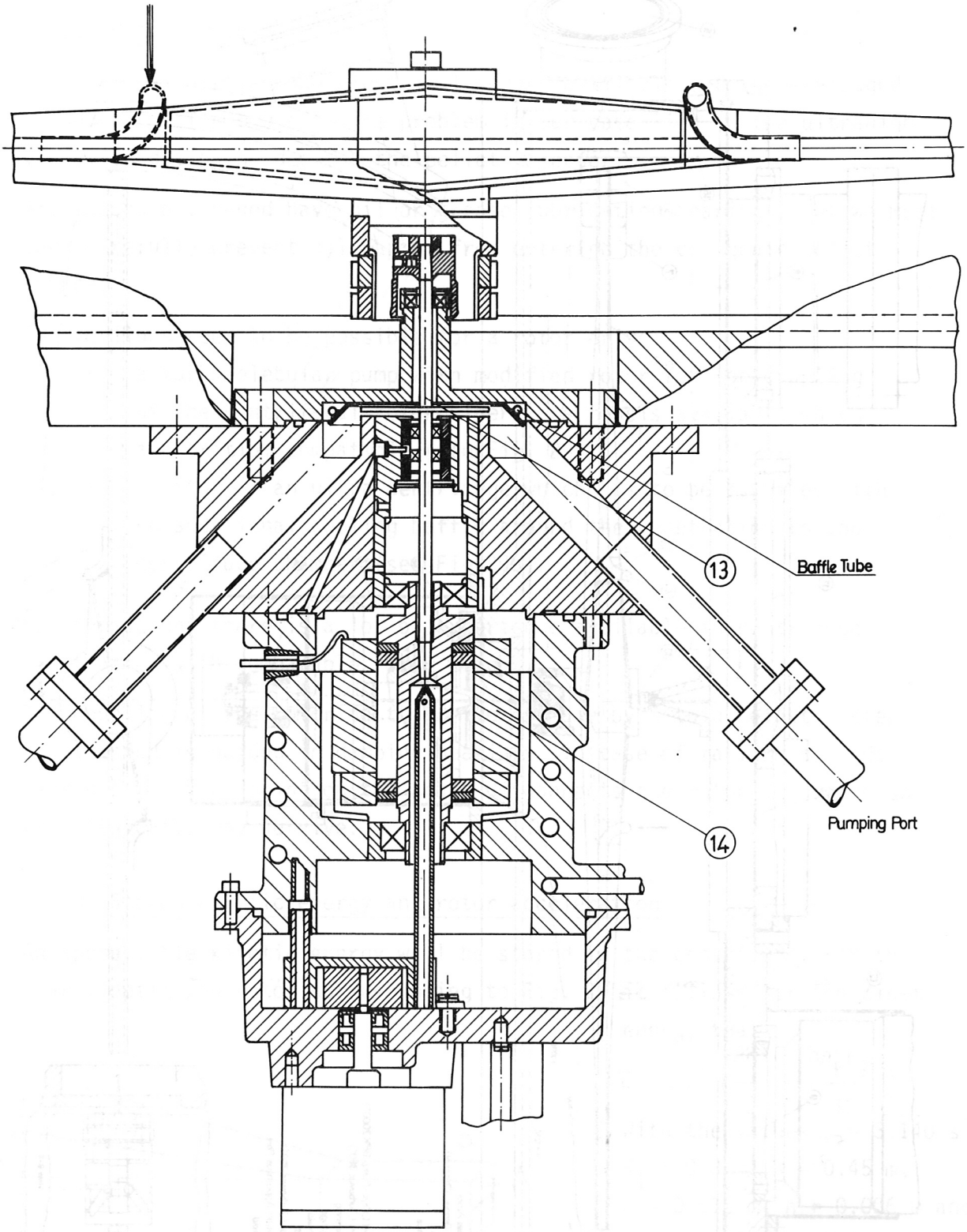

Fig.29b Beckman Centrifuge Drive Mod.L8-55

In addition, we have to expect an energy of the motor and the hub of about 35 kJ, therefore a total of about 250 kJ.

If we assume a driving power of N = 300 W, we can estimate a rotor acceleration time of

$$T = \frac{E_{kin}}{N} = \frac{250 \times 10^3}{300} = 833 \text{ s} \approx 14 \text{ min.}$$

4.3.4 Alternative shape of the centrifuge rotor

A completely different rotor shape was developed by the Oak Ridge pellet injection group (APS 1980). Figure 30 shows a schematic view of this rotor.

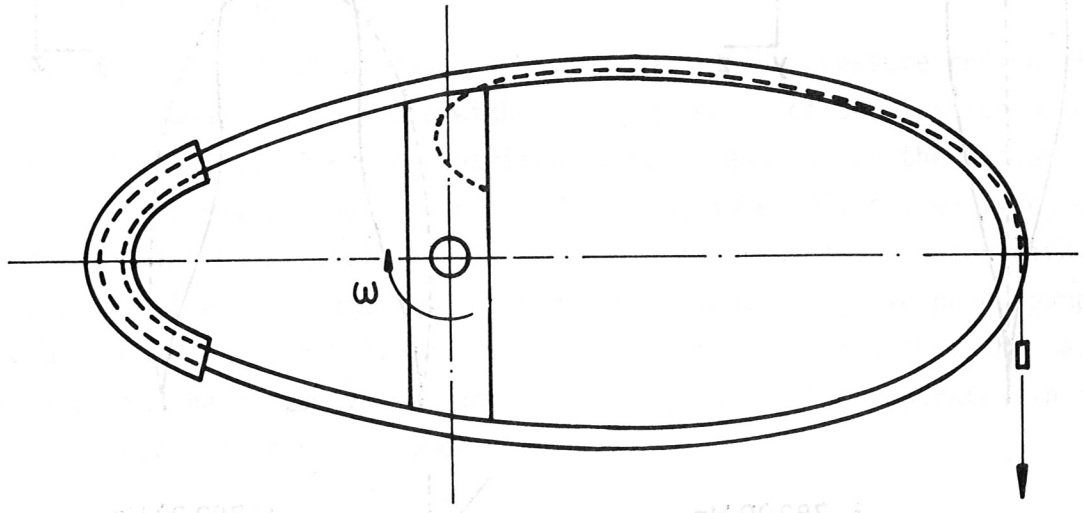

Fig. 30 Oak Ridge version of centrifuge rotor geometry

A Kevlar fibre ring with a special shape is supported by an aluminium spoke which has a much smaller radius than the ring at the pellet ejection point. The shape of the ring is such that during rotation there exist only tensile stresses in the material, but no shear or bending stresses. This looks very well adapted to the unidirectional strength of the Kevlar fibre ring. A further advantage could be that the pellet leaves the rotor tangentially and therefore with a velocity of 2 v_u instead of $\sqrt{2}\, v_u$. But the maximum tensile strength in the ring is the same as in the straight rod for a given pellet velocity.

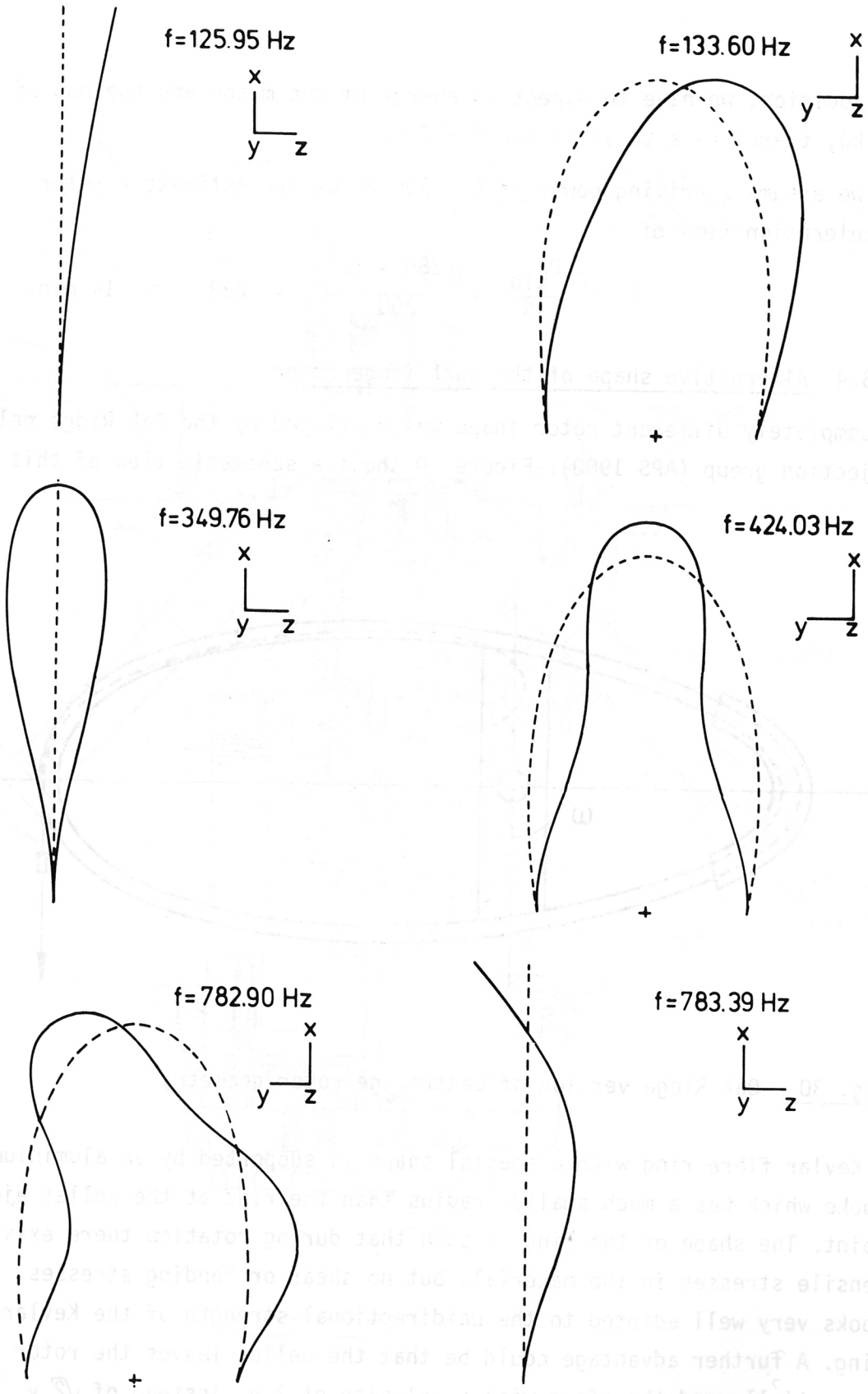

Fig.31 Oscillation modes of the Oak Ridge rotor

There are also disadvantages. The above-mentioned consideration of the stresses are only valid for rotation without oscillations. During acceleration we have to cross four resonances f = 126, 134, 350 and 424 s^{-1} (see Fig. 31), which introduce bending and shear stresses. Owing to the relatively high curvature especially at the largest radius the dynamic compression stress acting on the pellet is much higher than in the case of acceleration with the straight rod. The maximum tolerable dynamic compression stress for deuterium ice is not yet known.

These considerations lead us to the proposed pellet acceleration with a straight rod, which will also be easier to construct.

4.4 Vaccum and support system

The vacuum system must be capable of working in the pressure region of 10^{-7} mb. Turbomolecular pumps with a pumping speed of 340 l/s for H_2 are therefore envisaged for the centrifuge vacuum vessel, for the vacuum system of the pellet source and for the beam-guiding tube. Air-cooled types of turbomolecular pumps will facilitate remote maintenance. The centrifuge vacuum vessel will be equipped with an additional cryogenic pump (pumping speed is 6000 l/s for H_2). This is necessary in the event that the pellets are lost in the vacuum vessel and a large amount of D_2 evaporates in the vessel, which is at room temperature.

The vacuum vessel will have an inner diameter of 1000 mm and will be made of stainless steel (see Fig. 29). Inside will be a ceramic ring which is a suitable shielding against a bursting rotor. The opening to the beam-guiding tube should be as small as possible, but it depends on the spread angle of the pellets. Both sides of the beam-guiding tube should be provided with ultra-high vacuum valves.

The backing vacuum system will be part of the JET services.

The support structure will be fabricated from aluminium profiles corresponding to Fig. 32. The support can be adjusted and fixed in its final position. The pellet path lies at a height of about one meter. The space needed for the centrifuge and support will be about 3 m in length, 1.5 m for

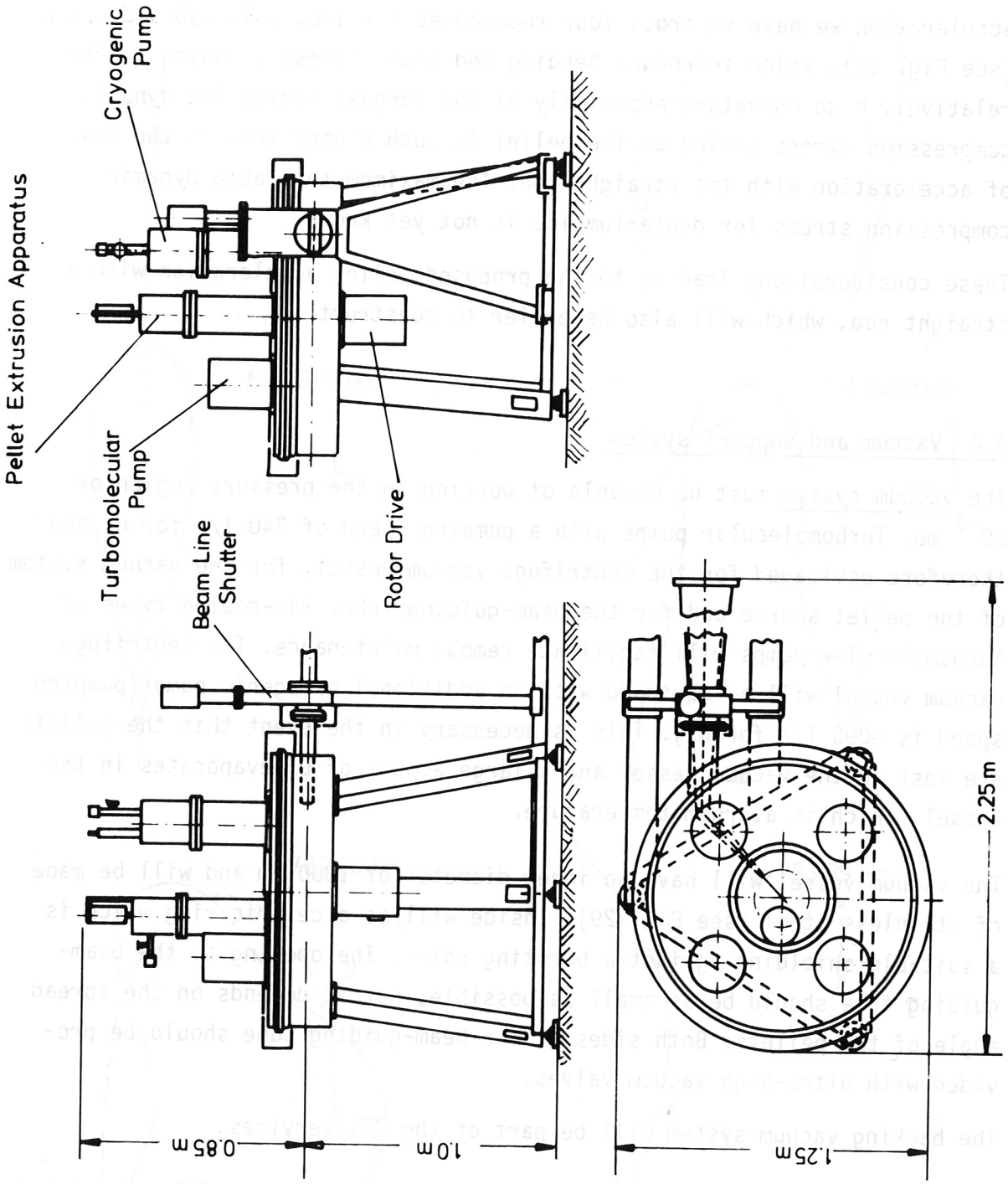

Fig.32 Total view of the centrifuge pellet injector

maintenance should be provided. This space could also serve for removable shielding in the DD and DT phases of JET.

The centrifuge can only be run with vertical rotation axis.

4.5 Control system

A scheme of the control system of the centrifuge pellet injector is shown in Fig. 33. A short description of the purposes of the different black boxes is given.

The central unit plays the dominant role. It contains all the timers for triggering D_2 ice production, ice formation, extrusion, and fast drive for the feed-in, synchronizes the cutter and resets and triggers parts of the diagnostics. Signals for pellet size and frequency should be delivered by JET operation central unit or by manual handling. The position of the central unit will be in the diagnostic control room.

The vacuum system control unit contents all vacuum surveying instruments, control units for all pumps, valves, and the cooling medium supplies for both cryostates and pumps. Safety circuits will prevent wrong operations, e.g. stopping the centrifuge in the event of a leak in the centrifuge vessel. An important role is played by the imbalance control of the centrifuge for possible prevention of complete rotor destruction.

The details of the black boxes are not elaborated except the control of the cryostat for pellet production, which will be the same as described in Sec. 3.5.

4.6 Cryogenic services

For the operation of the cryogenic devices liquid helium and nitrogen should be supplied by line. The quantities requires are:

1. pellet source: liquid He 10 l/h
2. cryogenic pump: liquid He 0.1 l/h plus
   2 l for cooling down
   liquid N_2 1 l/h

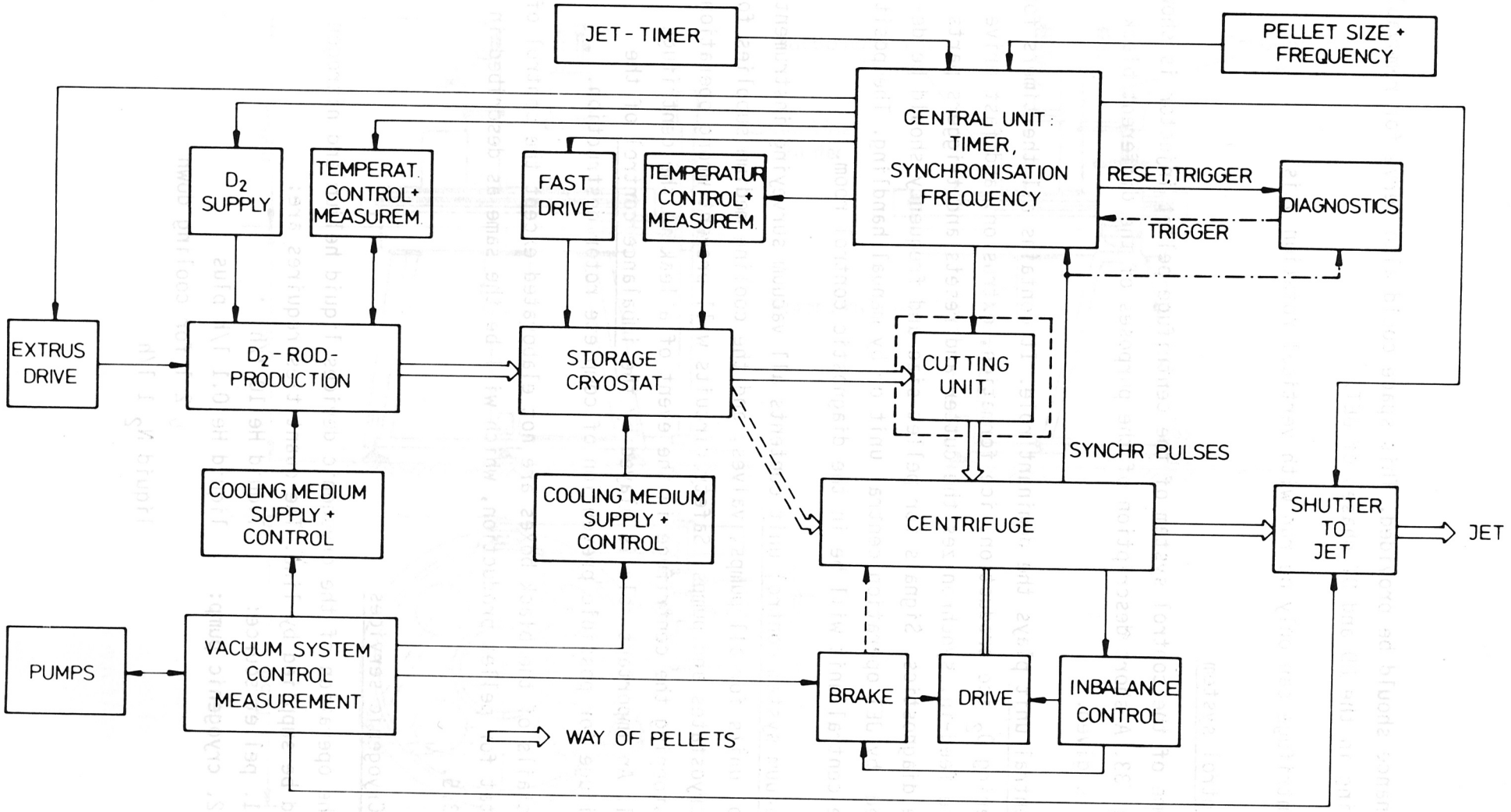

Fig.33 Control system of the centrifuge pellet injector

The pressure difference across the pellet source is about 500 mb.

The exhaust line for the helium circuit has to handle a helium flux at 7.5 m^3/h.

5. Pellet Diagnostics and Data Acquisition

5.1 General

Two different methods of pellet acceleration, the light gas gun and the centrifuge, are provided for pellet injection into the JET torus. Both devices are designed to produce deuterium pellets 2 - 4 mm in diameter and about 3 mm in length and to accelerate them to velocities of 300 - 2000 m/s. From the diagnostic point of view the two methods differ mainly in the pellet rate (100 pellets at rates of up to a few times 10 / s of the centrifuge compared with only one pellet of the light gas gun) and in the expected reproducibility of the path angle ($\pm 4^o$ for the centrifuge and $\pm 0.5^o$ for the light gas gun). The proposed pellet diagnostic system is based on the light gas scheme, which will be applied in an earlier phase of JET operation. The necessary modifications to adapt the system to the centrifuge accelerator are indicated in the text. Pellet properties to be measured by the diagnostic system are its acceleration time (light gas gun only), velocity, path angle and size.

5.2 Velocity and path angle measurement

The pellet velocity and the path angle are measured by an arrangement of two light barriers (each consisting of several channels) located at some distance. For the light gas gun the starting point of the pellet is well defined, and so an array of 10 light barrier channels each is adequate to measure the horizontal and vertical path angles with an accuracy of 0.11^o. In the case of the centrifuge accelerator the starting point in the horizontal direction is less reproducible, and therefore both light barriers are arranged in the horizontal direction with 64 channels each for a resolution of 0.15^o. Details of the location and optical layout are given in Sec.5.7.The time of flight between the barriers, which gives a

measure of the pellet velocity, is measured by a scaler (10 ms range with 1 μs resolution, clock frequency 1 MHz for the light gas gun and 2 MHz for the centrifuge) which is started and stopped by pulses from the light barriers. The start pulse of the first light barrier is also used to trigger the light pulse and start the readout of the camera used for the pellet size diagnostics.

The outputs of the light barriers and of the scaler are latched and converted into serial data strings of 128-bit length. This data is stored in a Camac memory together with camera signals of the pellet size diagnostics. The clock frequency of the serial converter is therefore synchronized with the horizontal scan of the camera. Since the light barrier and scaler data are not available when the camera readout starts, the serial converter is started with the second half-image of the camera. Loading of the data into the Camac memory is described in Sec. 5.3. In the case of the light gas gun independent displays of the path angle and time of flight are provided for immediate information of the operator without the need of computer backup. For the centrifuge a computer-based listing of experimental results can be obtained by using a local control console.

5.3 Pellet size measurement

The pellet size is evaluated from two shadow images of the pellet taken at 90^{o} which will be projected into one plane for recording by a TV camera. The pellet is irradiated by a laser pulse shortly after it has passed the first light barrier. Details of the optical layout are given in Sec. 5.7. To avoid problems with the magnetic field, a solid-state (charge coupled device) camera has been chosen which gives a resolution of 488 x 390 picture elements. This corresponds to a pellet size resolution of 0.1 mm for the light gas gun and 0.3 mm for the centrifuge owing to the larger image field of the centrifuge that is required.

For the information of the operator the NTSC video output of the camera controller is recorded on a NTSC compatible video tape recorder. In order to avoid synchronization problems between the camera and the video recorder, both have to be operated continuously for some seconds before

useful pictures can be recorded. Care has to be taken to avoid coincidence of the laser irradiation pulse and the photogate pulse of the camera, which would result in an undefined camera signal. The start of the pellet acceleration is therefore synchronised with the 60 Hz half-image frequency of the camera. The recorded picture is reproduced on a NTSC video monitor as a half-image or copied by a hard-copy device. In order to facilitate the search and identification of useful pictures on the video tape, the separate audio tracks are used to mark the events and to put out a consecutive pellet number. This recording method is applicable with pellet frequencies of up to 30 Hz. So far no practical and economical way has been found to store and record up to 100 pictures at rates higher than 30 Hz. The data acquisition of the pellet size, however, is not restricted by this frequency limit. In the data acquisition branch the high data flow of the camera is reduced to allow storage in a memory of moderate size. This is achieved by only counting the number of dark picture elements of each horizontal line of the camera. Although the pellet outlines are lost by this procedure, adequate information is preserved to evaluate the pellet volume by the computer. The binary output and the clock pulses of the camera are connected by a logic circuit to produce counting pulses for each line scan. The horizontal synchronization pulses of the camera are used to transfer the data and to reset the scaler at the end of each line. The logic circuit enlists for two complete half-images after a start impulse from the first light barrier. The output of the latching scaler requires only 9 bits of the 16-bit word length of the memory. The remaining bits can be used for other purposes. One bit is used to record vertical synchronization pulses for easier identification of the data. Two bits contain the serial data of the light barrier and the time of flight scaler. Another bit is enlisted for identification reasons when the serial converter for these signals is busy. In the case of camera malfunction an auxiliary pulse generator is provided to ensure storage of these signals.

5.4 Timing measurements

The acceleration time of the pellet in the light gas gun barrel, which is characteristic of the device performance and pellet quality, is measured

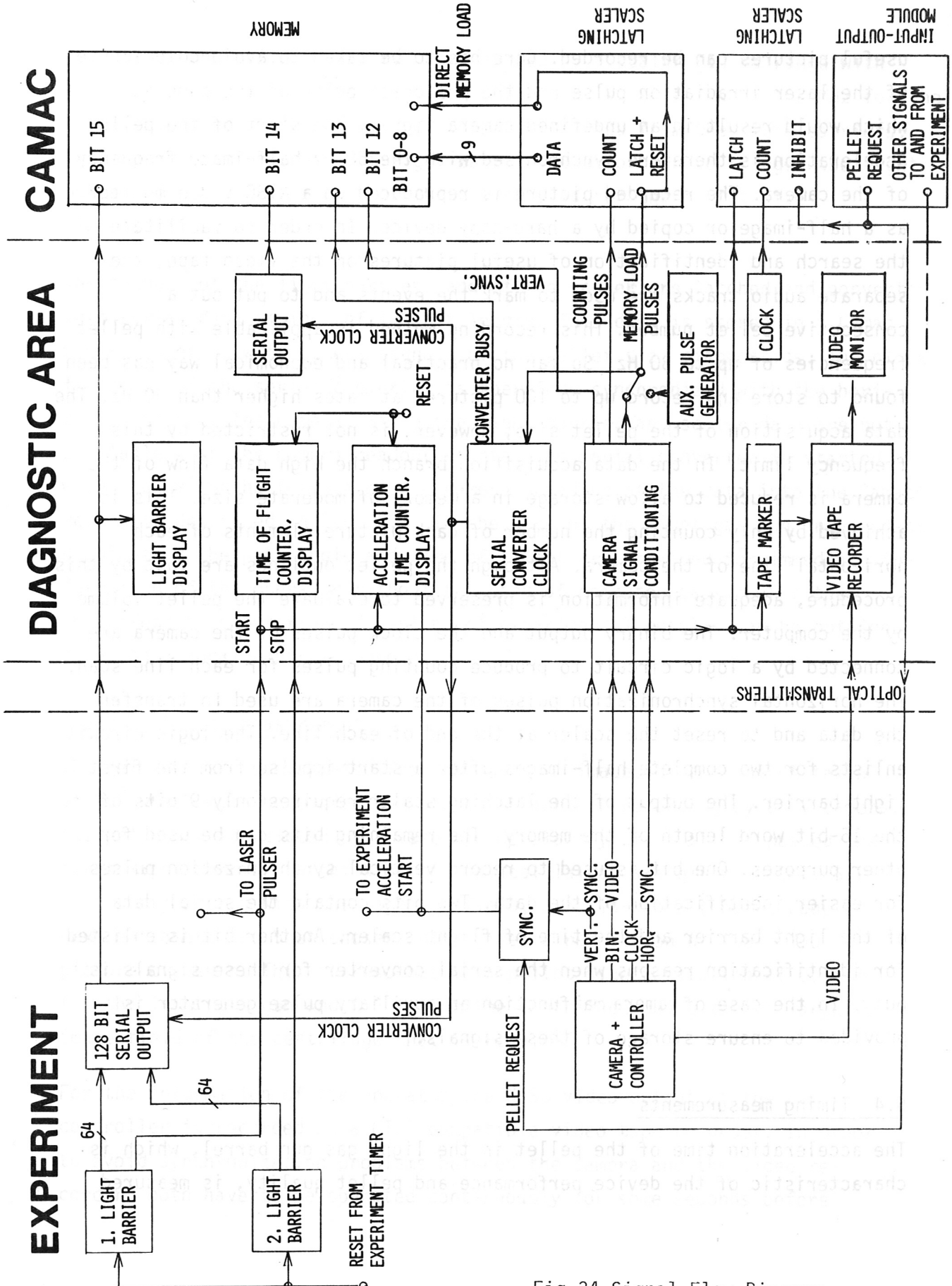

Fig.34 Signal Flow Diagram

by another scaler. This scaler is started when the light gas valve opens. When the pellet passes the first light barrier the counting direction is reversed until the scaler is stopped by the second light barrier pulse. This method has been chosen to cancel out the unaccelerated time of flight between the end of the gun barrel and the first light barrier. The acceleration time is displayed for the operator (10 ms range with 1 µs resolution at 1 MHz clock frequency) and is not stored by the data acquisition system. The time delay between the pellet request by the computer and the pellet delivery is measured by a second Camac scaler (655 ms range with 10 µs resolution at 100 kHz clock frequency) which is started by the pellet request signal and stopped by the first light barrier signal.

5.5 Camac interface

The Camac modules of the interface are selected to gather the data without the need of an auxiliary controller or of computer backup. Dual port memory modules have been chosen to store external data at successive memory locations with external write pulses. The latching scalers are adapted to this mode of operation. The stored data can be read out by the computer using the internal Camac port. The Camac interface for the light gas gun diagnostics consists of the Camac crate and the serial crate controller, one latching scaler and one memory module for the light barrier, time of flight and pellet size diagnostics, one latching scaler for the pellet delay signal and one input/output module. The input/output module is used to transmit the pellet request signal and for communication between the computer and the experiment before and after the discharge. For the higher data output of the centrifuge 4 memory modules have to be added, one for the timing signals and 3 for the other signals. The memories are cascaded using a memory selector which enlists the next module after a "memory filled" signal of the preceding module.

5.6 Signal flow and timing sequence

A signal flow diagram for the diagnostic system is given in Fig. 34. The timing sequence starts with a reset pulse from the experiment for the

counters and light barriers which also starts the video tape. After the pellet request signal (a few seconds later) which starts the time delay scaler the system waits for a vertical synchronization signal of the camera (0 - 16.7 ms) to initiate the light gas valve and the acceleration scaler. After 3 - 6 ms the pellet passes the first light barrier. The light barrier pulse starts the time of flight scaler, stops the time delay scaler, reverses the counting direction of the acceleration scaler and triggers the laser pulser which is delayed by 10 - 18 μs. With the next half image the data-reduced storage of the camera signal is started and continues for a complete image (33 ms). When the second barrier is passed, 0.5 - 3 ms after the first, the time of flight and acceleration scalers are stopped. The serial data of the scalers and the light barriers are transmitted, starting with the second half-image of the camera. After a few seconds the video tape is stopped. The readout and reset of the Camac components by the computer is initiated after the JET discharge.

5.7 Location and optical layout

The location of the light barriers has to be coordinated with the requirements of the vacuum system. For the light gas gun the distances between the end of the gun barrel and the first light barrier and between the first and the second light barrier are 90 cm each. For the centrifuge the distances have to be reduced to 13 cm between the flange connection and the first light barrier and to 50 cm between the two light barriers. The pellet size is measured near the first light barrier, so that pellets of different velocity are sure to be in the observed area when the laser pulse is applied.

For radiological reasons it is not advisable to locate sensitive devices such as semiconductors near the experiment. It is therefore planned to transmit the optical signals to the diagnostic area and to locate the necessary electronics there. Quartz glass has to be used for the optical components in order to avoid impairment of the transmission by transient and permanent radiation effects. The layout of the light barrier optics for the light gas gun is sketched in Fig. 35. The light source consists of

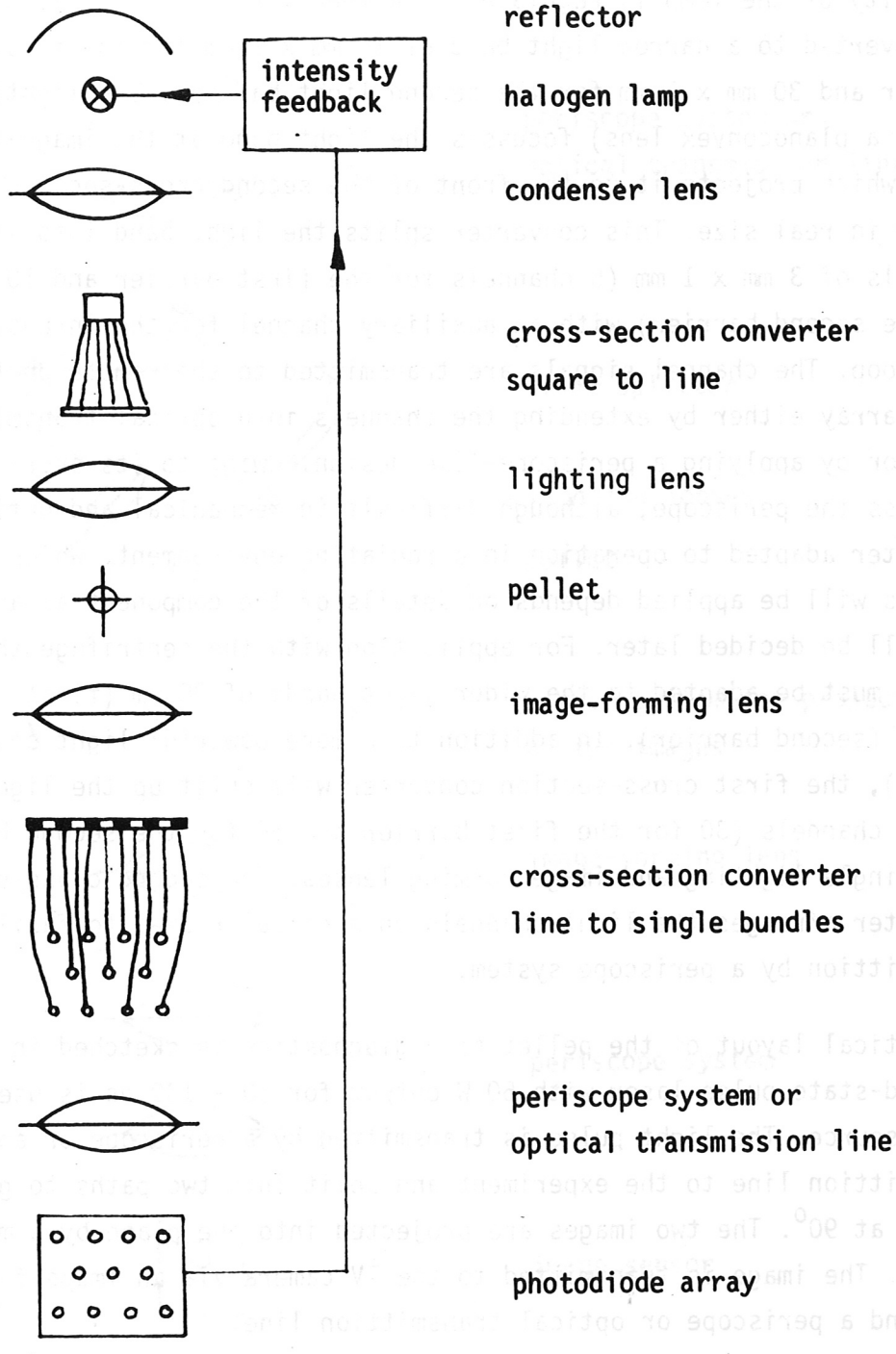

Fig.35 **Optical layout of the light barriers**

a 50 W halogen lamp with reflector mirror and condenser lens. The intensity of the lamp is regulated by a feedback loop. The light output is converted to a narrow light band of 15 mm x 1 mm for the first light barrier and 30 mm x 1 mm for the second light barrier. The lighting optics (using a planoconvex lens) focusses the light band at the image-forming lens, which projects it to the front of the second cross-section converter in real size. This converter splits the light band into single channels of 3 mm x 1 mm (5 channels for the first barrier and 10 channels for the second barrier) with an auxiliary channel for the intensity feedback loop. The channel signals are transmitted to the remote photo- (PIN)-diode array either by extending the channels into optical transmission lines or by applying a periscope-like design. Owing to its short light paths in glass the periscope, although difficult in mechanical and optical layout, is better adapted to operation in a radiating environment. Which of the two schemes will be applied depends on details of the component arrangement and will be decided later. For application with the centrifuge the optical system must be adapted to the wider light bands of 90 mm (first barrier) and 160 mm (second barrier). In addition to a more powerful light source (115 W), the first cross-section converter will split up the light into single channels (30 for the first barrier and 54 for the second barrier) with single lighting and image-forming lenses. The second cross-section converter arranges the light channels on a circular area to facilitate transmittion by a periscope system.

The optical layout of the pellet size diagnostics is sketched in Fig. 36. A solid-state pulse laser with 50 W output for 50 - 100 ns is used as a light source. The light pulse is transmitted by a periscope or an optical transmittion line to the experiment and split into two paths to get two images at 90^{o}. The two images are projected into one plane by a mirror system. The image is transmitted to the TV camera via an image-forming lens and a periscope or optical transmittion line.

5.8 Grounding and signal decoupling

The inputs of the diagnostic devices have no connection to experiment ground. The light barrier electronics and the camera system are grounded

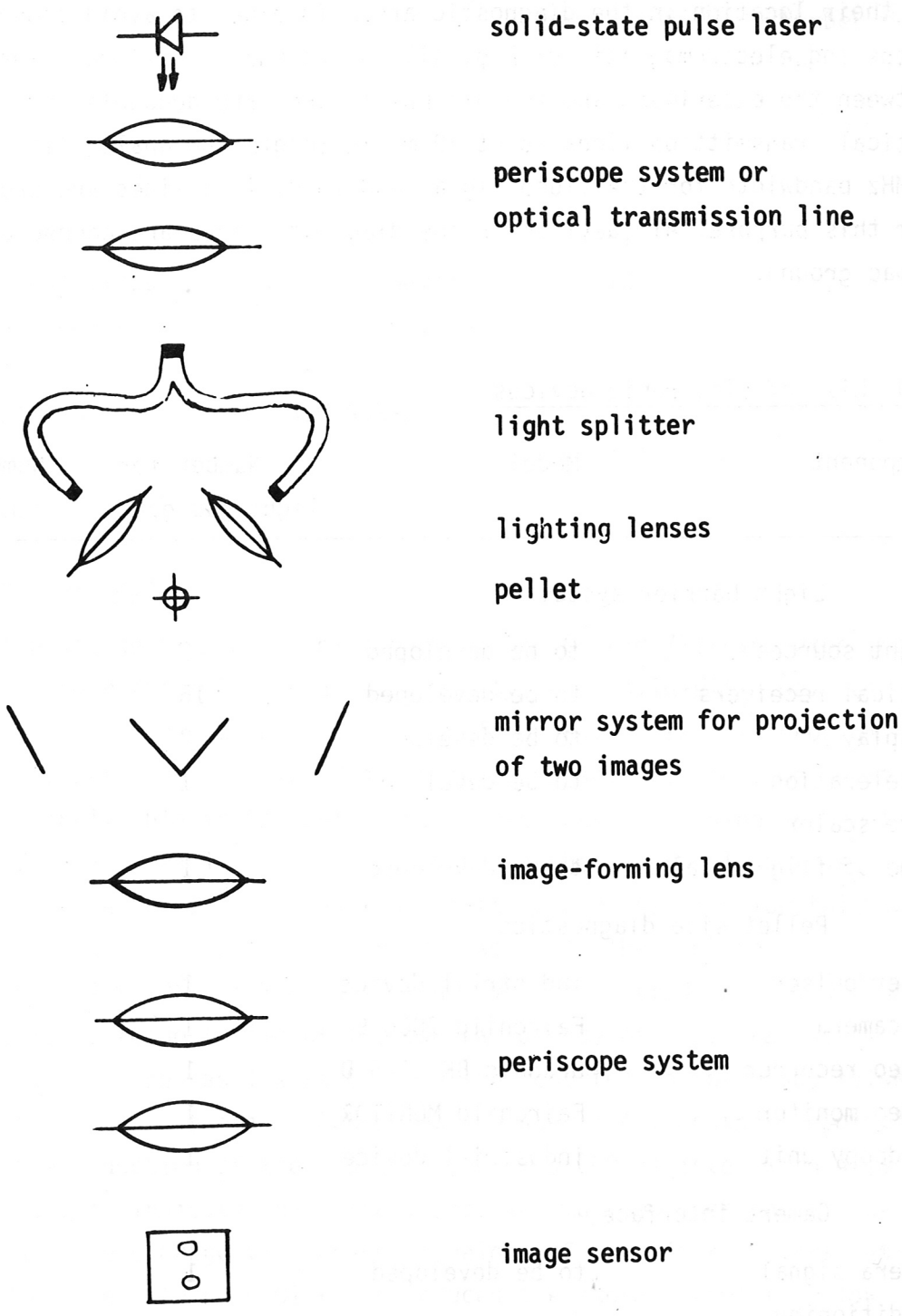

Fig.36 **Optical layout of the pellet size diagnostics**

at their location in the diagnostic area. In order to avoid ground loops and electromagnetic pickup, all interconnecting signal lines between the experiment and the diagnostic area are decoupled by optical transmittion lines about 30 m in length. An analog line of 6 MHz bandwidth for the video signal and 10 digital lines are provided for this purpose. All devices in the diagnostic area are connected to Camac ground.

5.9 List of electronic devices

Component	Model	Number for light gas gun	Number for centrifuge
Light barrier system			
Light sources	to be developed	2	2
Optical receivers	to be developed	15	84
Display	to be developed	2	2
Acceleration Time scaler	to be developed	1	-
Time of flight scaler	to be developed	1	1
Pellet size diagnostics			
Laser pulser	industrial device	1	1
TV camera	Fairchild 2000 C	1	1
Video recorder	Grundig BK 2145 D	1	1
Video monitor	Fairchild MONITOR	1	1
Hardcopy unit	industrial device	1	1
Camera interface			
Camera signal conditioning	to be developed	1	1
I/O module	Dornier Do 200-2815	1	1
Latching scalers	Le Croy 8590	2	2
Memory modules	Le Croy 8801/16	1	5
Memory selector	to be developed	-	1
Camac crate	Grenson CPC/29	1	1
Serial crate contr.	GEC-Elliott SCC2401	1	1

Component	Model	Number for light gas gun	Number for centrifuge
Miscellaneous			
Timing controller	to be developed	1	1
Optical signal lines	industrial device	12	12
cables and connectors, racks	industrial device		
Power suppliers	AEC-NIM NÜR-G	4	6

6. Radiological Implications

In the D-T phase neutron doses of the order of 10^7 rad /11/ are expected at locations near the pellet source. Since typical solid-state devices are permanently damaged by neutron doses of 10^4 rad, /12/ this problem is exemplified for the pellet size diagnostics by a solid-state camera. It will not be applicable in the D-T phase unless heavy shielding or remote location of the camera is considered. Although the camera element is likely to survive the 10^3 rad neutrons of the D-D phase, its low tolerance to transient radiation must be taken into account. The neutron dose of 10^3 rad corresponds to 4×10^3 rad γ - radiation which is emitted in 7500 s /13/. During the 33 ms readout time of the camera a dose of 0.018 rad is accumulated. γ - doses as low as 0.1 rad are reported to introduce false data into a digitally operated CCD shift register /14/. Another reported effect is the reduction of the storage time of a CCD register with dose rate /15/. The results indicate that with a zero accumulated dose and a dose rate of 0.03 rad/s the storage time drops to below 500 ms. After an irradiation of 10^3 rad a dose rate of 0.01 rad/s reduces the storage time to below 500 ms. On the basis of the previous assumptions our dose rate is 0.53 rad/s. Although our storage time is only 33 ms, these results show that our operating conditions are close to the device limits. Shielding or remote location of the camera is therefore necessary even in the D-D phase.

Similar considerations are valid for solid-state circuits in control units of the cryogenic devices, the vacuum system and the drive for pneumatic or centrifugal acceleration.

The vacuum connection to the JET torus will only be open as briefly as possible. The tritium influx will therefore be minimized. UHV systems will ensure tritium tightness. Lubrication of the turbomolecular pumps is to be done with Fomblin. The exhaust of the vacuum systems will be connected with the tritium-compatible JET manifold vacuum line.

7. Time Schedule after Beginning of Phase I

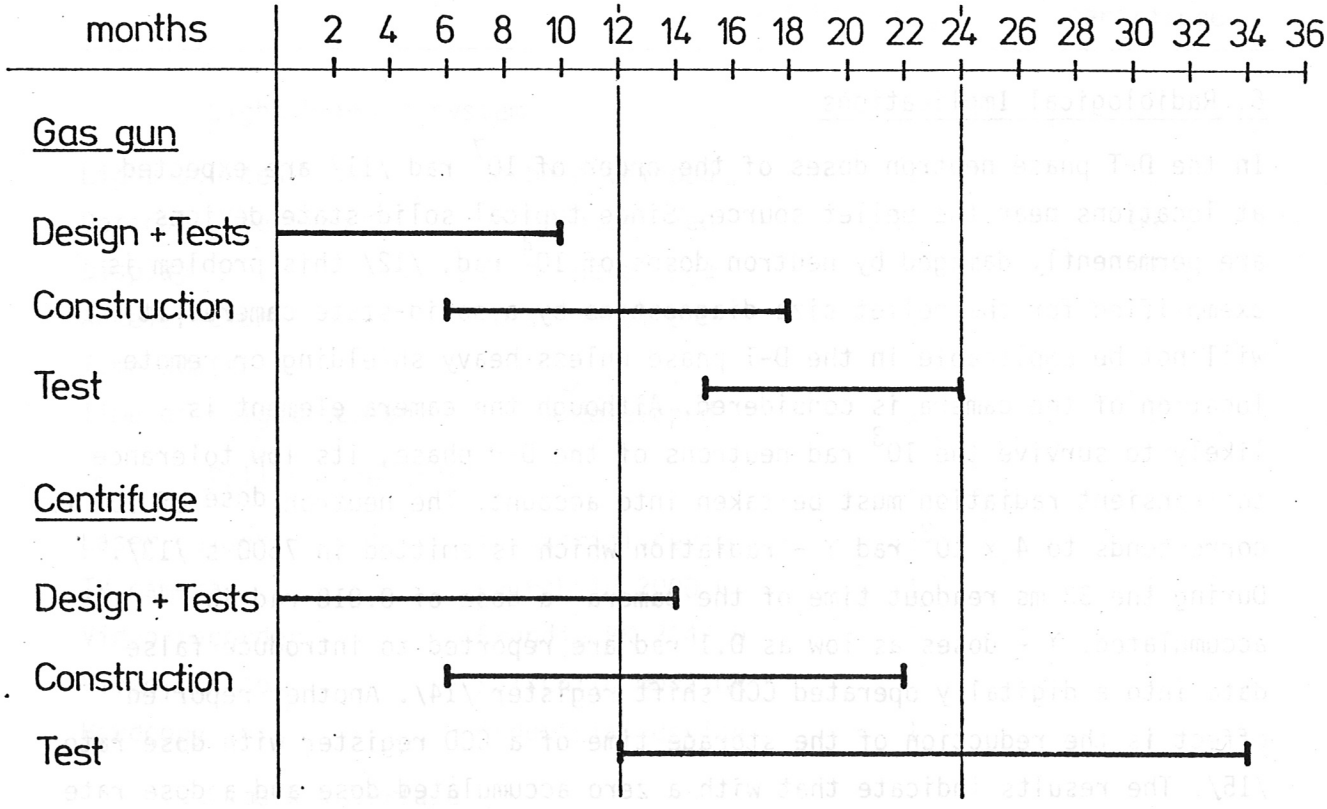

References

/1/ L. Spitzer, D.J. Grove, W.E. Johnson, L. Tonks and W.F. Westendorps, USAEC Report NYO-6047 (1954)

/2/ S.L. Milora, Journal of Fusion Energy, Vol. 1, p. 15 (1981)

/3/ P.B. Parks, R.J. Turnbull and C.A. Foster, Nucl. Fusion 17, 539 (1977)

/4/ S.L. Milora, C.A. Foster, Oak Ridge Nat. Lab. Report, ORNL/TM-5776 (1977)

/5/ C.I. Chang, L.W. Jørgensen, P. Nielsen, L.L. Lengyel, The feasibility of pellet re-fuelling of a fusion reactor, Nucl. Fus. 20 (7), 859 (1980)

/6/ W.A. Houlberg, M.A. Iskra , H.C. Howe, S.E. Attenberger, Pellet - a computer routine for modeling pellet fuelling in tokamak plasmas, ORNL/TM-6549 (1979)

/7/ Landau-Lifschitz, Lehrbuch der theoret. Physik VI, Hydrodynamik, Berlin 1966, p. 419

/8/ C.A. Foster, S.L. Milora, Bull. Am. Phys. Soc. 23, 790 (1978)

/9/ C.A. Foster, S.L. Milora, DOE CONF-771129, p. 117 (1978)

/10/ W. Amenda, R.S. Lang, Max-Planck-Institut für Plasmaphysik, IPP-Report 1/187 (1981)

/11/ W. Amenda, R.S. Lang, to be published in Cryogenics

/12/ P. Noll, JET Radiation Levels ... JDN/H (1980) 12

/13/ S. Battisti et al., Radiation damage to electronic components, Nucl.Instruments and Methods 13b (1976)

/14/ A. Gibson, JET Radiation Levels and their consequences

/15/ W. Shedd, B. Buchmann, Transient Radiation Effects in CCD's, IEEE Transactions on Nucl.Science, Vol.NS-23, No.6 (1976)

/16/ G.J. Bruckner, Radiation damage effects ..., TFTR Diagnostics Engineering Report, PH-I-004